

**EFFECT OF FINES CONTENT ON CPT
RESISTANCE IN SILTY SANDS**

**A Thesis Submitted to
the Graduate School of Engineering and Sciences of
İzmir Institute of Technology
in Partial Fulfillment of the Requirements for Degree of**

MASTER OF SCIENCE

in Civil Engineering

**by
Mustafa Sezer ARIK**

**April 2021
İZMİR**

ACKNOWLEDGMENTS

I would like to special thanks to my supervisor Assoc. Prof. Dr. Nurhan ECEMIŐ ZEREN, who helped me take part in this scientific study, guided me in the planning, research and execution of my thesis, gave me self-confidence in scientific terms with her knowledge and experience, and never withheld her patience and understanding.

I would like to express my special thanks to the jury members Dr. Volkan İŐBUŐA and Prof. Dr. Murat MONKUL for participating in the thesis defense seminar and their valuable suggestions for this study.

I would like to special thanks to my father Salih ARIK, who always wanted me to follow the path of science and supported me in all circumstances, and my mother Nurdoėan ARIK, who always stood by me with all his means and never spared his efforts.

My special thanks to my dear sisters Sezen Burcu ARIK and Selen Duygu ARIK, whose support and love I always feel by my side.

Special thanks to Mustafa KARAMAN and my teammates Murat ÖRÜCÜ, Ceren Gizem SARITAŐ, Hazal TANERİ and Ali Hamid KHLAIF for their support and contribution to my laboratory studies.

ABSTRACT

EFFECT OF FINES CONTENT ON CPT RESISTANCE IN SILTY SANDS

The effect of fines content on cone penetration resistance and excess pore water pressure is not entirely known yet. In this study, CPTu, SCPT, and DPPT tests in a fixed wall laminar box were carried out to understand the effect of fines content with different relative densities on cone penetration resistance and excess pore water pressure in clean sand and sand with 5, 15, and 35 percent silty. This study was investigated by using the normalized penetration rate. The effect of normalized penetration rate accounted with penetration rate and coefficient of consolidation on drainage conditions and the value of transition from partially drained to drained conditions were investigated.

According to the experimental data results, the effect of fines content on the coefficient of volume compressibility is minimal. However, as the fines content increase, the permeability and the coefficient of consolidation decrease considerably. The normalized cone penetration resistance decreases when the fines content increases in clean sand and silty sands at the same relative densities. When the relationship between normalized penetration rate and normalized cone penetration resistance is examined instead of only the fines at the same relative densities, the normalized cone penetration resistance decreased with the increasing normalized penetration rate. Due to a decrease in the coefficient of consolidation or an increase in the penetration rate, silty sands have a longer dissipation time of excess pore water pressure than clean sand. Hence, the clean sand remains drained, and the silty sands remain partially drained.

ÖZET

SİLTİLİ KUMLARDA İNCE DANE MUHTEVASININ CPT DİRENCİNE ETKİSİ

İnce dane muhtevasının koni penetrasyon direnci ve aşırı boşluk suyu basıncı üzerindeki etkisi henüz tam olarak bilinmemektedir. Bu çalışmada, temiz kum ve yüzde 5, 15 ve 35 siltli kumlarda farklı relatif sıklılıklara sahip ince dane muhtevasının koni penetrasyon direnci ve aşırı boşluk suyu basıncı üzerindeki etkisini anlamak için sabit duvarlı laminer kutuda CPTu, SCPT ve DPPT testleri gerçekleştirilmiştir. Bu çalışma normalleştirilmiş koni penetrasyon hızı ile araştırılmıştır. Penetrasyon hızı ve konsolidasyon katsayısı ile hesaplanan normalize penetrasyon hızının drenaj koşulları üzerindeki etkisi ve kısmen drenajlı koşullardan drenajlı koşullara geçiş değeri araştırılmıştır.

Deneyel veri sonuçlarına göre, ince dane muhtevasının hacim sıkıştırılabilirlik katsayısı üzerindeki etkisi minimumdur. Ancak ince dane muhtevası arttıkça geçirgenlik ve konsolidasyon katsayısı önemli ölçüde azalır. Normalleştirilmiş koni penetrasyon direnci, aynı relatif sıklılıklarda temiz kum ve siltli kumlarda ince dane muhtevası arttığında azalır. Normalize penetrasyon hızı ile normalize koni penetrasyon direnci arasındaki ilişki, sadece aynı relatif sıklılıklardaki ince dane muhtevasının yerine incelendiğinde, normalize penetrasyon hızının artması ile normalize koni penetrasyon direnci azalmıştır. Konsolidasyon katsayısındaki düşüş veya penetrasyon hızındaki artış nedeniyle, siltli kumlar, temiz kuma göre aşırı boşluk suyu basıncını daha uzun sönmüleme süresine sahiptir. Bu nedenle, temiz kum drenajlı olarak kalır ve siltli kumlar kısmen drenajlı halde kalır.

TABLE OF CONTENTS

LIST OF FIGURES	vii
LIST OF TABLES.....	x
CHAPTER 1 INTRODUCTION	1
1.1. Introduction and Scope of Study.....	1
1.2. Thesis Organisation	2
CHAPTER 2 LITERATURE REVIEW	4
2.1. Introduction.....	4
2.2. Normalized Cone Penetration Resistance and Normalized Excess Pore Water Pressure	5
2.3. The Effect of Fines on Coefficient of Volume Compressibility and Permeability and Coefficient of Consolidation in Silty Sands	5
2.4. Normalized Penetration Rate (T).....	7
2.5. Conclusion.....	14
CHAPTER 3 BOX SETUP AND SAMPLE PREPARATION FOR LABORATORY TESTS	15
3.1. Introduction.....	15
3.2. Laminar Box Setup	15
3.3. Sample Preparation	18
3.4. Properties of Sample	28
3.5. Conclusion	31
CHAPTER 4 LABORATORY TESTS	32
4.1. Introduction.....	32
4.2. Piezocone Penetration Test (CPTu).....	33
4.2.1. Historical Development of CPTu.....	33

4.2.2. Test Equipment	34
4.2.3. Test Procedure.....	37
4.2.4. CPTu Test Data	38
4.3. Seismic Cone Penetration Test (SCPT)	42
4.3.1. Test Equipment	42
4.3.2. Test Procedure.....	43
4.3.3. SCPT Test Data.....	46
4.4. Direct Push Permeability Test (DPPT)	48
4.4.1. DPPT Test Data	49
4.5. Conclusion	51
CHAPTER 5 RESULTS OF THE TESTS	52
5.1. Introduction.....	52
5.2. m_v , k and c_h of Clean Sand and Silty Sands at Different Relative Densities.....	52
5.3. Effect of Fines Content and Relative Density on Normalized Cone Penetration Resistance and Normalized Excess Pore Water Pressure.....	59
5.4. Effect of Coefficient of Consolidation and T on q_{c1N} and $\Delta u/\sigma_{v0}'$	62
5.5. Conclusion	66
CHAPTER 6 CONCLUSION	67
REFERENCES	69

LIST OF FIGURES

<u>Figure</u>	<u>Page</u>
Figure 2.1. (a) Effect of fines on k (b) effects of fines on c_v (c) effect of fines on m_v (d) effects of fines on $(c_v)_o/(c_v)$. (Source: Thevanayagam and Martin, 2002)	6
Figure 2.2. The effect of relative density on the cone resistance in different fines content (Source: Kokusho, 2012).....	10
Figure 2.3. The effect of normalized penetration rate on normalized cone penetration resistance. (Source: Huang, 2015)	11
Figure 2.4. The effect of normalized penetration rate on normalized excess pore water pressure. (Source: Huang, 2015).....	12
Figure 2.5. (a) Permeability versus cone penetration resistance (b) the permeability versus excess pore water pressure. (Source: Markauskas, 2005)	12
Figure 2.6. (a) The effect of T on $\Delta u/\sigma'_{vo}$ (b) the effect of T on q_{c1N} (Source: Ecemis, 2008)	13
Figure 3.1. (a) Schematic view of the top, side and front of the wheeled platform system, (b) construction of the wheeled platform system in the plant.....	16
Figure 3.2. Laminar box platform.....	17
Figure 3.3. Laminar box (160 cm length, 150 cm depth and 40 cm width)	17
Figure 3.4. Sample preparation box (155 cm length 77 cm wide).....	18
Figure 3.5. (a) Weighed sample (b) Funnel system for the dry filling of sample.....	19
Figure 3.6. Densification plate.....	19
Figure 3.7. Sample preparation process in each layer for (a) loose clean sand (b) medium dense clean sand (c) dense clean sand	20
Figure 3.8. Sample preparation process in each layer for 5% silty sands (a) loose (b) dense (c) medium dense	21
Figure 3.9. Sample preparation process in each layer for 15% silty sands (a) loose (b) medium dense (c) dense.....	22
Figure 3.10. Sample preparation process in each layer for 35% silty sands (a) loose (b) dense (c) medium dense (d) dense.	23

<u>Figure</u>	<u>Page</u>
Figure 3.11. The samples laid in thin layers on the linoleum to dry	25
Figure 3.12. (a) CO ₂ gas source system (b) pneumatic hoses inserted under the box c) 2 mm diameter holes for homogeneous distribution (d) The mechanism for giving CO ₂ gas into the sample	26
Figure 3.13. SEM view of (a) clean sand (b) 5% silty sand (c) 15% silty sand (d) 35% silty sand samples at 400 μm resolution	28
Figure 4.1. Locations of CPTu, SCPT, DPPT tests in the box.	33
Figure 4.2. Figure 4.2. (a) The Wissa piezometer probe (b) filter element position	34
Figure 4.3. (a) Piezocone and Nova (b) Probe with a cable adapter and Rod	35
Figure 4.4. (a) Data acquisition system (b) Interface Box (Source: CPT Geotech NOVA MANUAL, 2015)	36
Figure 4.5. Hydraulic pushing system.	36
Figure 4.6. The CPTu experiment performed in the laboratory.	37
Figure 4.7. (a) The cone resistance (b) pore water pressure data of clean sand with the penetration depth for Test 1, Test 2 and Test 3.....	38
Figure 4.8. (a) The cone resistance (b) pore water pressure data of 5% silty sand with the penetration depth for Test 4, Test 5 and Test 6.....	39
Figure 4.9. (a) The cone resistance (b) pore water pressure data of 15% silty sand with the penetration depth for Test 7, Test 8 and Test 9.....	40
Figure 4.10. (a) The cone resistance (b) pore water pressure data of 35% silty sand with the penetration depth for Test 10, Test 11 and Test 12.....	41
Figure 4.11. SCPT data acquisition system (Source: Holmsgaard et al. Interpretation of Seismic Cone Penetration Testing in Silty Soil, 2016).....	43
Figure 4.12. (a) Sledgehammer (b) Steel plate (c) Seismic data acquisition box.....	43
Figure 4.13. The SCPT experiment performed in the laboratory	44
Figure 4.14. GeoTech SCPT Analysis program by performing the CrossCorrelation method.....	45
Figure 4.15. The shear wave velocity data of (a) clean sand (b) 5% silty sand (c) 15% silty sand (d) 35% silty sands, with the penetration depth.....	47
Figure 4.16. (a) A filter is placed at the cone's tip, allowing water to flow out (b) Cylindrical water reservoir, water and gas inlet and valves.	48

<u>Figure</u>	<u>Page</u>
Figure 5.1. The relative density versus coefficient of compressibility in clean sand and silty sands.	55
Figure 5.2. c_h values of clean sand, 5%, 15%, and 35% silty sands according to fines content.	57
Figure 5.3. c_h values with respect to relative densities in fines content.	58
Figure 5.4. Relative density versus normalized cone penetration resistance in clean sand and 5%, 15% and 35% silty sands.	61
Figure 5.5. Relative density versus normalized excess pore water pressure in clean sand and 5%, 15% and 35% silty sands.	61
Figure 5.6. Comparison of T with qc_{1N} at given relative densities.	64
Figure 5.7. Comparison of T with $\Delta u/\sigma'_{vo}$ at given relative densities.	64

LIST OF TABLES

<u>Table</u>	<u>Page</u>
Table 2.1. The transition value of T in drained and undrained conditions.	8
Table 2.2. The cone resistance values were measured for CPT were conducted between 0.1 mm/sec and 0.02 mm/sec penetration rates (Kumar and Raju, 2009).....	9
Table 3.1. CO ₂ gas pressure and application of CO ₂ gas given in the experiments.	27
Table 3.2. Physical properties of sand and silty sands (Source: Saritas, 2021).....	29
Table 3.3. For the clean sand samples prepared, the weight of the solid, water weight, calculated total volume, water content, density, void ratio (e) and relative density (D _r).....	30
Table 3.4. For the 5% silty sand samples prepared, the weight of the solid, water weight, calculated total volume, water content, density, void ratio (e) and relative density (D _r).....	30
Table 3.5. For the 15% silty sand samples prepared, the weight of the solid, water weight, calculated total volume, water content, density, void ratio (e) and relative density (D _r).....	30
Table 3.6. For the 35% silty sand samples prepared, the weight of the solid, water weight, calculated total volume, water content, density, void ratio (e) and relative density (D _r).....	31
Table 4.1. The modified DPPT permeability data. (Source: Saritas, 2021).	50
Table 5.1. m _v values calculated according to Equation 5.5 at different depths and different relative densities.....	54
Table 5.2. c _h values at different depths and different relative densities.	56
Table 5.3. q _{c1N} and Δu/σ _{vo} ', the parameters used to calculate q _{c1N} and Δu/σ _{vo} '.	60
Table 5.4. T and its parameters (v, c _h), q _{c1N} and Δu/σ _{vo} ' values at different depths and different relative densities in clean sand and 5%, 15% and 35% silty sands.....	63

CHAPTER 1

INTRODUCTION

1.1. Introduction and Scope of Study

The Cone Penetration Test (CPT) determines the geotechnical properties and boundaries of the soil. CPT has essential advantages in geotechnical engineering as it offers rapid and continuous profiling, reliability, and repeatability. However, the effect of fines on cone penetration resistance and excess pore water pressure in the CPT is a prominent problem. The effect of fines content on the coefficient of volume compressibility (m_v), permeability (k), and coefficient of consolidation (c_h) have been investigated in very few studies. Researchers have found that clean sand compared with silty sands, have very different k and c_h values (Shenthan, 2001; Thevanayagam and Martin, 2002; Ecemis, 2008; Bandini and Sathiskumar, 2009; Huang, 2015). The coefficient of consolidation is an essential soil parameter in the time of generation and dissipation of pore water pressure in cone penetration and affects drainage conditions. Limited experimental and numerical data have been reported in the literature to quantify the impact of the coefficient of consolidation on cone penetration resistance and excess pore water pressure. Researchers show that in addition to the coefficient of consolidation, the penetration rate and diameter of the cone also affect the cone penetration resistance and the excess pore water pressure. For this, it has been suggested to use T , which is defined as the normalized penetration rate that varies depending on penetration rate (v), the diameter of the cone (d), and coefficient of consolidation (c_h). (Finnie and Randolph, 1994; House et al., 2001; Randolph and Hope, 2004; Chung et al., 2006; Kim et al., 2008; Ecemis, 2008).

The research was conducted to examine the limit values for the normalized penetration rate during cone penetration with clay for undrained conditions (Kim et al., 2008; Jaeger et al., 2010; Oliveira et al., 2011; Yi et al., 2012) with silty sands. (Ecemis, 2008; Kumar and Raju, 2009; Kokusho et al., 2012; Huang, 2015). However, the effect of fines content

on cone penetration resistance and excess pore water pressure is not clear enough. Therefore, the effect of the CPT-based fines content should be understood better by the relationship between the T-normalized cone penetration resistance and the T-normalized excess pore water pressure.

In this study, in order to understand the effect of fines content on cone penetration resistance and excess pore water pressure, samples of clean sand and 5%, 15%, and 35% silty sands were prepared with different relative densities as fully saturated with water. The CPTu, SCPT, and DPPT tests were performed in a fixed-wall laminar box to provide experimental data and to assess the effect of fines content directly. Experiments aim to understand the effect of T on the normalized cone penetration resistance and normalized excess pore water pressure with different penetration rates and coefficients of consolidation. Determination of the transition values of T from drained to partially drained aimed to be found.

1.2. Thesis Organisation

In the thesis, there are six Chapters: Introduction, Literature Review, Box Setup and Sample Preparation for Laboratory Tests, Laboratory Tests, Results of The Tests, and Conclusion.

Chapter 2 presents experimental and numerical studies on the effect of fines content on cone penetration resistance and excess pore water pressure in silty sands.

Chapter 3 presents the preparation of the fixed-wall laminar box and preparation of test specimens that are fully saturated with water.

Chapter 4 presents the laboratory tests (CPTu, SCPT, and DPPT), test equipment, test procedures and standards, and data obtained from the tests.

Chapter 5 presents the investigation of normalized cone penetration resistance and normalized excess pore water pressure in clean sand and silty sands in permeability, coefficient of volume compressibility, coefficient of consolidation, relative density, fines content, and penetration rate. Detailed interpretations of the normalized cone penetration

resistance and the normalized excess pore water pressure with different coefficients of consolidation, penetration rate, fines content, and relative density are also provided.

In Chapter 6, the concluding part and suggestions for further studies are examined.

CHAPTER 2

LITERATURE REVIEW

2.1. Introduction

The effect of fines content on cone penetration resistance and excess pore water pressure in silty sands is not fully understood, even though more studies have been carried out over the past several years. The effect of drainage conditions on cone penetration resistance and excess pore water pressure has been the subject of very few research. In CPT's numerical and experimental studies, studies were conducted on clean sand for drained conditions (Van Den Berger, 1994; Kumar and Raju, 2009) and clay for undrained conditions. (Kioussis, 1988; Schneider et al., 2007).

Permeability, coefficient of volume compressibility, and coefficient of consolidation of clean sand and silty sands have been the subject of several studies (Shenthan, 2001; Thevanayagam and Martin, 2002). The effect of fines content on the drainage conditions in silty sands was explored by taking the penetration rate and cone diameter into account as well as the coefficient of consolidation (Finnie and Randolph, 1994; House et al., 2001; Randolph and Hope, 2004; Chung et al., 2006; Kim et al., 2008; Ecemis, 2008).

Firstly, the effect of fines content on permeability, coefficient of volume compressibility, and coefficient of consolidation in silty sands are presented in this Chapter. Then, the effect of fines content in silty sands on normalized cone penetration resistance and normalized excess pore water pressure is discussed with numerical and experimental studies on T. Besides, the effect of fines content on drainage conditions and T limit values for both drained and undrained conditions are presented.

2.2. Normalized Cone Penetration Resistance and Normalized Excess Pore Water Pressure

Some studies have been performed to investigate the effect of fines content on cone penetration resistance and excess pore water pressure. In these studies, normalized cone penetration resistance (q_{c1N}) and normalized pore water pressure ($\Delta u/\sigma_{v0}'$) were used, and these parameters are explained as follows.

$$q_{c1N} = \frac{q_{c1}}{P_a} = C_Q \left(\frac{q_c}{P_a} \right) \quad (2.1)$$

$$C_Q = \left(\frac{P_a}{\sigma_{v0}'} \right)^m \quad (2.2)$$

$$m = 0.784 - 0.521D_r \quad (2.3)$$

where q_{c1N} is the normalized cone penetration resistance, P_a is the atmospheric pressure, q_c is the cone penetration resistance from the field, C_Q is the correction factor for cone penetration resistance, σ_{v0}' is the initial effective vertical overburden pressure, and m is the factor based on soil density. (Boulanger, 2003).

$$\frac{\Delta u}{\sigma_{v0}'} = \left(\frac{u_2 - u_0}{\sigma_{v0}'} \right) \quad (2.4)$$

where $\Delta u/\sigma_{v0}'$ is the normalized excess pore water pressure, u_2 is the measured pore water pressure on the cone, u_0 is the hydrostatic pore water pressure, and σ_{v0}' is the initial effective vertical pressure overburden pressure. (Schneider et al., 2007).

2.3. The Effect of Fines on Coefficient of Volume Compressibility and Permeability and Coefficient of Consolidation in Silty Sands

Thevanayagam and Martin (2002) used Ottawa sand and Ottawa sand-silt mixture of fines content of 15%, 25%, 40%, 60%, and 100%. Coefficient of consolidation and permeability affected by an equivalent relative inter-granular density ($(D_{rc})_{eq}$) determined by the fines content was examined in these experiments.

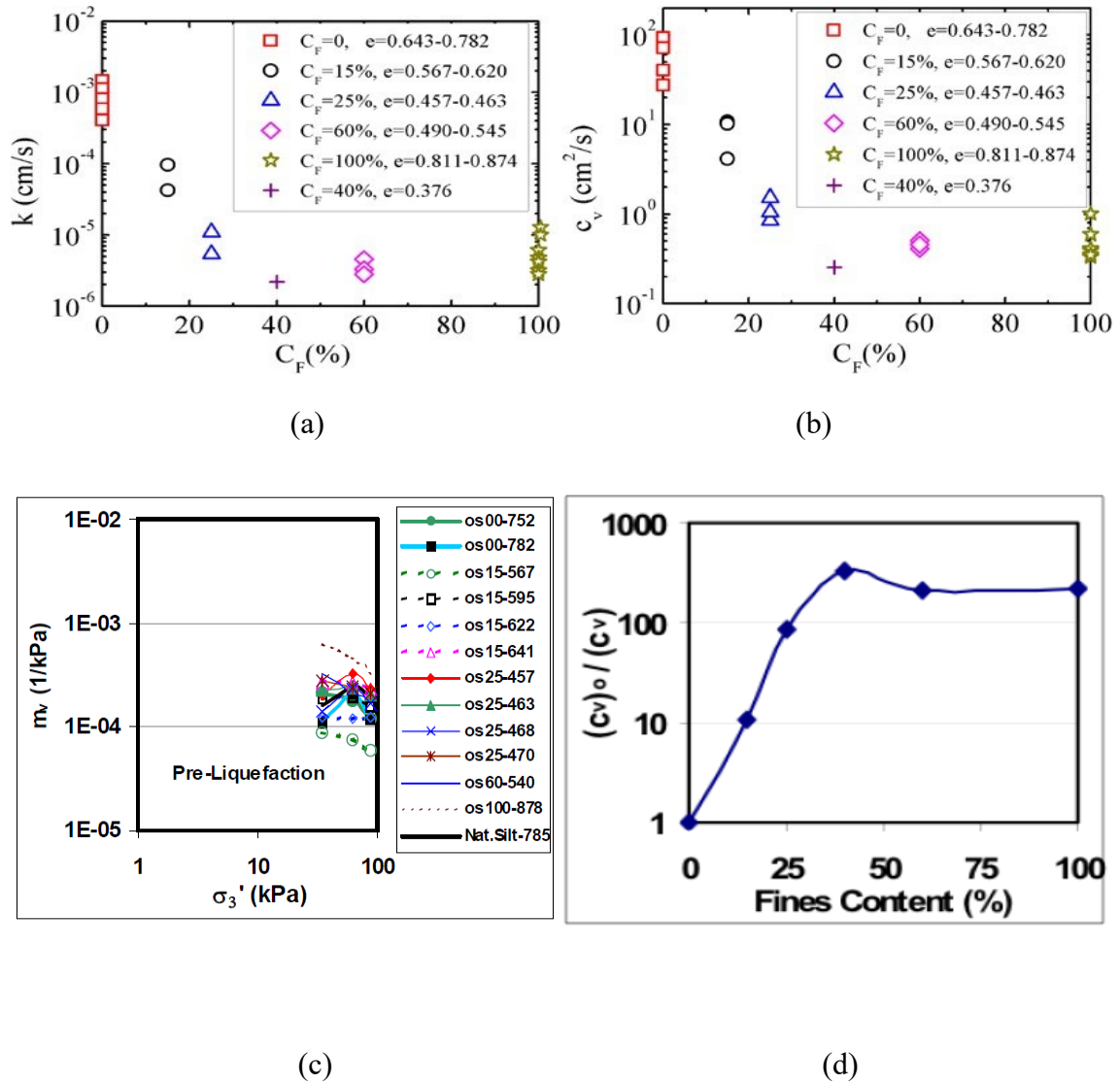


Figure 2.1. (a) Effect of fines on k (b) effects of fines on c_v (c) effect of fines on m_v (d) effects of fines on $(c_v)_o / (c_v)$ (Source: Thevanayagam and Martin, 2002)

In Figure 2.1. (a) and 2.1. (b), permeability and coefficient of consolidation values are compared with fines content. $FC = 60\%$ and $e = 0.490-0.545$ given in the graphs means that the fines content is 60% and the void ratio ranges from 0.490 to 0.545. When the silt ratio increases by up to 40%, there is a significant decrease in permeability and coefficient of consolidation due to the decrease in the void ratio. After passing the threshold value (40%) in the silt ratio, a slight increase is observed in permeability and coefficient of consolidation as the void ratio increases. In Figure 2.1. (c), coefficient of volume compressibility (m_v) and confining stress are compared with various silt ratios. 'os60-540' means that the sample has 60% silt content and a 0.540 void ratio. The coefficient

of volume compressibility varies depending on the silt ratio. It is found in the diagram that the impact of the silt ratio on the coefficient of volume compressibility is negligible, contrasted with the impact on permeability. In Figure 2.1. (d), comparison of $(c_v)_0/c_v$ regarding fines content at same contact density $(e_c)_{eq}$ is shown. In the Figure, $(c_v)_0$ refers to the coefficient of consolidation of Ottawa sand, and c_v refers to the coefficient of consolidation of the Ottawa sand-silt mixture. While $(c_v)_0/c_v$ shows a significant increase as the silt ratio increases to the threshold value. The silt ratio increases after the limit threshold value are influenced $(c_v)_0/c_v$ insignificantly.

It has been seen in the observations that, with the same $(D_{rc})_{eq}$ and $(e_c)_{eq}$ values, fines content has a significant effect on permeability and coefficient of consolidation. Permeability and coefficient of consolidation values are lower in silty sands contrasted with sands. The difference in the coefficient of consolidation in the sand and silty sands influences the dissipation of the excess pore water pressure and causes different drainage conditions.

2.4. Normalized Penetration Rate (T)

The difference of permeability and coefficient of consolidation in sands and silty sands affects the dissipation time of excess pore water pressure, which causes diverse drainage conditions. Generally, CPT penetration is undrained in clays and drained in sands. Because of the high permeability and coefficient of consolidation of the clean sand, excess pore water pressure is generated and dissipates quickly. On the other hand, in clays, the abundance of excess pore water pressure dissipates very slowly because of the low permeability and coefficient of consolidation. The grain size of silts is between the grain size of sands and clays so, permeability and coefficient of consolidation are intermediate values in silts compared with sand and clays. CPT penetration in silty sands could be partially drained. The cone penetration resistance and excess pore water pressure in CPT depend on the fines content's drainage conditions. In studies that were done for the drainage conditions of silty sands, $T=vd/c_h$ was recommended.

$$T = \frac{v * d}{c_h} \quad (2.5)$$

where T is the normalized penetration rate, v is the penetration rate, d is the diameter of the cone, and c_h is the coefficient of consolidation (Finnie and Randolph, 1994; House et al., 2001; Randolph and Hope, 2004; Chung et al., 2006; Kim et al., 2008; Ecemis, 2008).

Some researches have been performed to determine the limit value of T in drained and undrained conditions. The transition values of T in these studies are given in the Table 2.1.

Table 2.1. The limit value of T in drained and undrained conditions

Type of Tests	Type of Soil	Undrained	Drained	References
Centrifuge	Sand	$T > 30$	$T < 0.01$	Finnie and Randolph, 1994
Centrifuge	Kaolin clay	$T > 10$	$T < 0.1$	House et al., 2001
Calibration chamber	Clayed sand	$T > 10$	$T < 0.05$	Kim et al., 2008
Numerical	Silty sand	$T > 6$	$T < 0.01$	Ecemis, 2008
Centrifuge	Kaolin clay	$T > 3-12$	$T < 0.05$	Lehane et al., 2009
Centrifuge	Clayed sand	$T > 20$	$T < 0.01$	Jaeger et al., 2010
Centrifuge	Clayed soil	$T > 70$	$T < 1$	Oliveira et al., 2011
Numerical	Fine-grained soil	$T > 10$	$T < 0.1$	Yi et al., 2012
Calibration Chamber	Silty Sand	$T > 10$	$T < 0.04$	Huang, 2015

Experimental and numerical researches were carried out to observe the effect of T on cone resistance. In experimental studies, Kumar and Raju (2009), Kokusho et al. (2012), and Huang (2015) investigations; in numerical studies, Huang (2015) and Ecemis (2008) investigations are explained.

Placing a 19.5 mm diameter miniature cone penetrometer in a 140 mm diameter triaxial chamber, Kumar and Raju (2009) conducted three soil surveys of varying penetration rates of clean sand, 15% silty sands, and 25% silty sands. In the mechanism, confining stress was once utilized at 100 kPa and 300 kPa.

The cone resistance values measured for CPT were conducted between 0.1 mm/sec and 0.02 mm/sec penetration rates that are given in the Table 2.2. As shown in the Table 2.2.'s values, the cone resistance increased with the increment of the penetration rate. The fact that the maximum penetration rate applied in the study was 0.1 mm/sec causes only drained conditions to be determined on the soil. However, it was found that it may no longer be enough for the transition from drained conditions to partially drained and undrained conditions, so the standard penetration rate of 20 mm/sec ought to be applied.

Table 2.2. The cone resistance values were measured for CPT were conducted between 0.1 mm/sec and 0.02 mm/sec penetration rates (Kumar and Raju, 2009)

Soil Type	$\sigma_{vo}'=100$ kPa	$\sigma_{vo}'=300$ kPa
Loose Clean Sand	12.7	8.4
Medium Dense, Clean Sand	8.2	6.3
Dense, Clean Sand	7.6	6.4
Loose 15% Silty Sands	10.5	8.0
Medium Dense 15% Silty Sands	8.8	7.0
Dense 15% Silty Sands	6.5	7.2
Loose 25% Silty Sands	15.9	14.9
Medium Dense 25% Silty Sands	13.2	11.8
Dense 25% Silty Sands	10.0	7.5

Kokusho (2012) carried out undrained triaxial exams with a miniature cone of 6 mm diameter and 115.2 mm height. The samples used in these assessments are 100 mm in diameter and 200 mm in height.

The impact of relative density on the cone resistance in distinct fines content is shown in Figure 2.2. $FC = 15\%$ and $CC = 0$ given in Figure 2.2., means that the fines content is 15% and the cement content is 0. While relative density increases, cone penetration resistance will increase in every fines content as well. It is observed in the Figure 2.2. that the cone resistance decreases as the fines content increases at the equal relative density.

The fines content varies from 0 to 30% in the experiments carried out in silty and clayey sands with a cone diameter of one-sixth of 35.7 mm, and the penetration rate is 0.2 cm/sec, one-tenth of the standard penetration rate. Therefore, it has caused the soil to be partially drained or even drained with the maximum fines content. Furthermore, the impact of the penetration rate on fines content no longer needs to be considered.

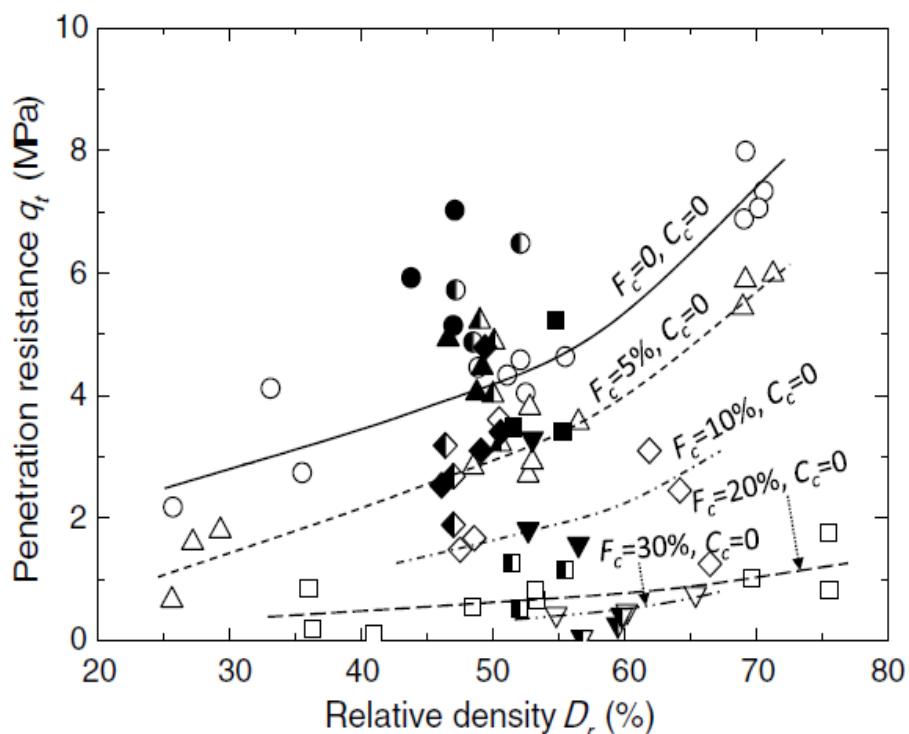


Figure 2.2. The effect of relative density on the cone resistance in different fines content
(Source: Kokusho, 2012)

Huang (2015) examined the effect of sands containing 0%, 15%, and 25% silt on cone resistance with a calibration chamber test. Using Ottawa F55 sand, a dry and fully saturated silt-sand mixture was once used with a 1.27 cm diameter cone for the tests with penetration rate vary from 0.09 cm/sec to 0.4 cm/sec for normalized penetration rate. Besides using the modified Drucker-Prager model for silty sands, the impact of normalized penetration rate on cone resistance is studied numerically. In the Ottawa F55 silty sand mixture at different relative densities, the effect of normalized penetration rate on normalized cone penetration resistance is given in Figure 2.3. The effect of normalized penetration rate on normalized excess pore water pressure is given in Figure 2.4. $(D_{rc})_{eq} = 60$ given in the Figure 2.3. and Figure 2.4. means that the relative density is 60.

Since silty sands have lower coefficients of consolidation than sand, it is seen that silty sands have a greater normalized penetration rate and lower normalized cone penetration resistance at a given relative density in the Figure 2.3. Hence, silty sands remain in partially drained or undrained conditions, and sand remains in drained conditions.

Since silty sands remain in partially drained conditions, they are affected with penetration rate (v) and diameter (d). Limit values have been determined in the study as $T < 0.04$ for drained conditions and as $T > 10$ for undrained conditions.

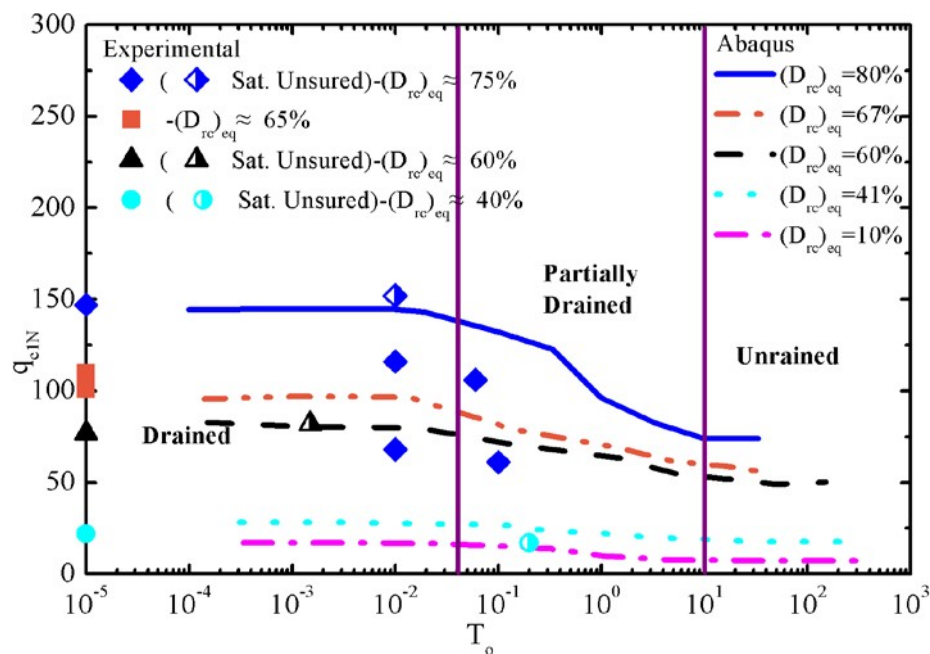


Figure 2.3. The effect of normalized penetration rate on normalized cone penetration resistance (Source: Huang, 2015)

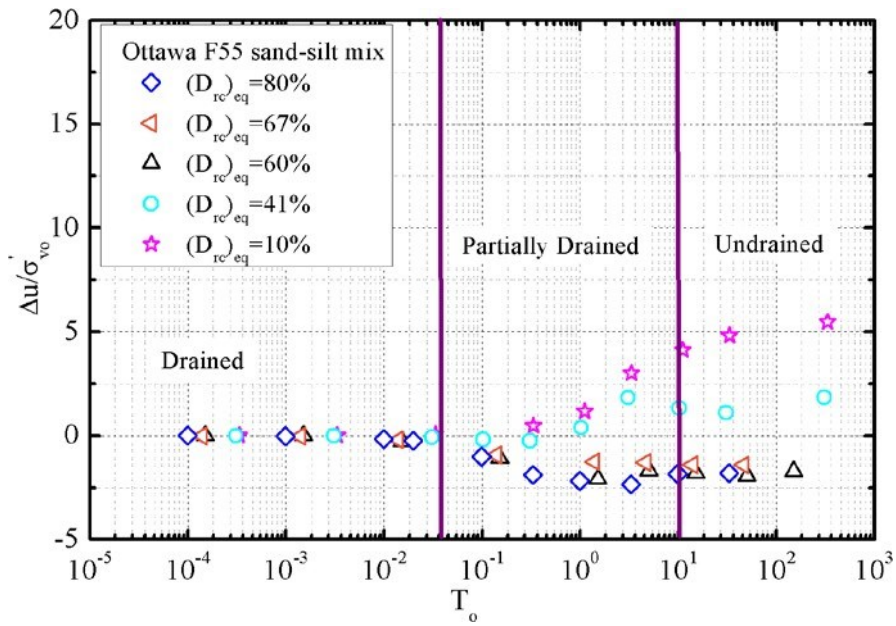


Figure 2.4. The effect of normalized penetration rate on normalized excess pore water pressure (Source: Huang, 2015)

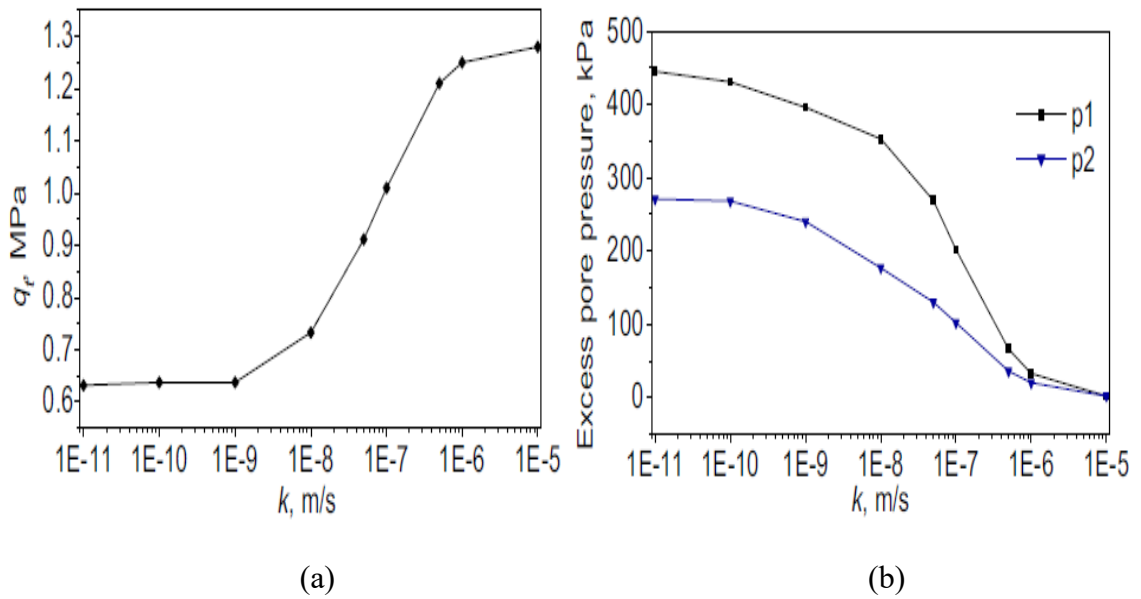


Figure 2.5. (a) Permeability versus cone penetration resistance (b) the permeability versus excess pore water pressure (Source: Markauskas, 2005)

Markauskas (2005) used the standard cone penetrometer with a diameter of 35.7 mm, a cone tip angle of 60 degrees, and a penetration speed of 2 cm/sec, modeled with a modified Drucker-Prager.

In Figure 2.5 (a) permeability and cone penetration resistance, in Figure 2.5 (b), the permeability and excess pore water pressure values are compared. As can be seen in Figures 2.5 (a) and (b), the limit value measured as $k < 10^{-9}$ for undrained, $k > 10^{-6}$ for drained, and $10^{-9} < k < 10^{-6}$ for partially drained conditions.

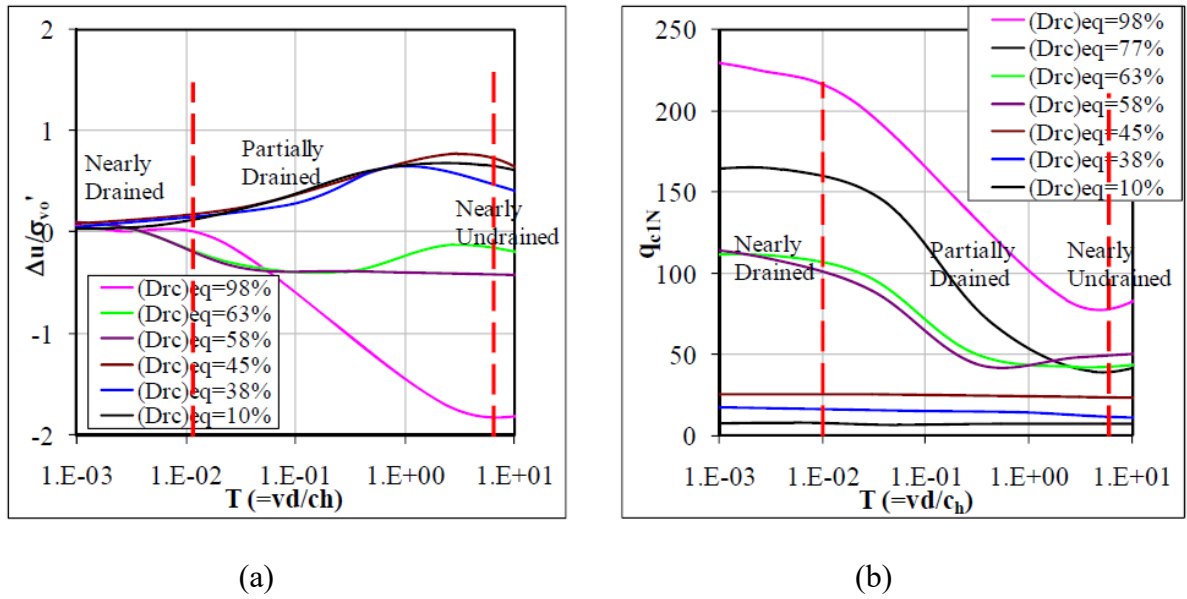


Figure 2.6. (a) The effect of T on $\Delta u/\sigma'_{v0}$ (b) the effect of T on q_{c1N}
(Source: Ecemis, 2008)

Ecemis (2008) investigated the impact of fines content via simulating the CPT with Drucker-Prager modeling on OF55 silty sands with cone diameter $d = 4.37$ cm and penetration rate $v = 2$ cm/sec. By examining the effect of fines content on k and c_h , it has been stated that the normalized cone resistance and the normalized excess pore water pressure rely on T in the given $(D_{rc})_{eq}$.

In Figure 2.6. (a), the effect of T on $\Delta u/\sigma'_{v0}$ is analyzed. It has been reported that $\Delta u/\sigma'_{v0}$ is low and changes minimally at $T < 0.05-0.01$ values and $\Delta u/\sigma'_{v0}$ is high and changes minimally at $T > 5-10$ values. It is seen that $\Delta u/\sigma'_{v0}$ is affected for the T values between 5 and 0.01 under partially drained conditions. In Figure 2.6. (b), the effect of T on q_{c1N} is analyzed. It has been reported that at $T > 5-10$, q_{c1N} is low and changes minimally; at $T < 0.05-0.01$ values, q_{c1N} is high and changes minimal, and between 5 and 0.01 T is under partially drained conditions.

Since k and c_h are lower in silty sands than clean sand, silty sands are partially drained or undrained, showing that q_{c1N} is lower in silty sands. Transition values of T have been determined as 0.01 for drained conditions and 6 for undrained conditions.

2.5. Conclusion

Fines content has a significant effect on q_{c1N} and $\Delta u/\sigma'_{vo}$. The difference between k and c_h of silty sands compared to clean sand affects the dissipation time of excess pore water pressure. Therefore, different drainage conditions occur with loading. The effect of fines content on q_{c1N} and $\Delta u/\sigma'_{vo}$ should be considered as $T = vd/c_h$. In each (Drc)eq drained and undrained conditions, as T increases, q_{c1N} and $\Delta u/\sigma'_{vo}$ are affected practically nothing. However, under part of the partially drained conditions, q_{c1N} decreases and $\Delta u/\sigma'_{vo}$ is affected as T increments. Studies in the literature determine the T limit value for drained and undrained conditions, and further studies are required. The following Chapter presents box setup and sample preparation for laboratory experiments..

,

CHAPTER 3

BOX SETUP AND SAMPLE PREPARATION FOR LABORATORY TESTS

3.1. Introduction

In this Chapter, the laminar box setup and sample preparation for laboratory tests are explained. Firstly, the laminar box was designed to be used as a fixed wall. For doing this, the wheeled platform system was prepared in the atelier and the laminar box installed on it. The laminar box consists of the laminates placed on top of each other and fixed with screws. A whole of thirteen tests have been carried out on clean sand, sand containing 5% of silt by weight and sand containing 15% of silt by weight, and sand containing 35% of silt by weight. For each of the clean sands and 5%, 15%, and 35% of silty sands, tests were prepared as loose, medium dense, and dense. While the mixing process was not utilized for clean sand, silty sands were homogeneously mixed and filled into the laminar box using the dry filling methodology. It was aimed to entirely saturate the samples via giving CO₂ gas before giving water to the filled sample. The relative density was evaluated using the samples recorded with the weight of solid and weight of water and physical properties.

3.2. Laminar Box Setup

A fixed wall laminar box with dimensions of 160 cm length, 150 cm depth and 40 cm width has been prepared for the experiments. First, a wheeled platform system was needed to construct below the laminar box to install the laminar box in the laboratory. The schematic views of the top, front, and side of the platform in Figure 3.1 (a) and the construction of the wheeled platform system in the atelier are given in Figure 3.1 (b). For the construction steps, steel profiles were welded to 6 cm cross-section and 199.5 cm

lengths profiles by slicing ten pieces of 6 cm cross-section and 66 cm lengths profiles. Then, the platform was welded longitudinally in both directions with 2 mm sheet metal. Four of them are movable and 360 degrees rotatable, and two of them are fixed. Six rubber wheels that can lift 2500 kilograms in total were installed under the platform. In Figure 3.2, holes were drilled in the wheeled platform system with massive drills to connect the wheeled platform system to the laminar box platform. After the screw wheeled platform system to the laminar box, each laminate was placed in a row and fixed. When the laminar box installation shown in Figure 3.3 was completed, a 1mm thick membrane was placed inside the laminar box to prevent water leakage.

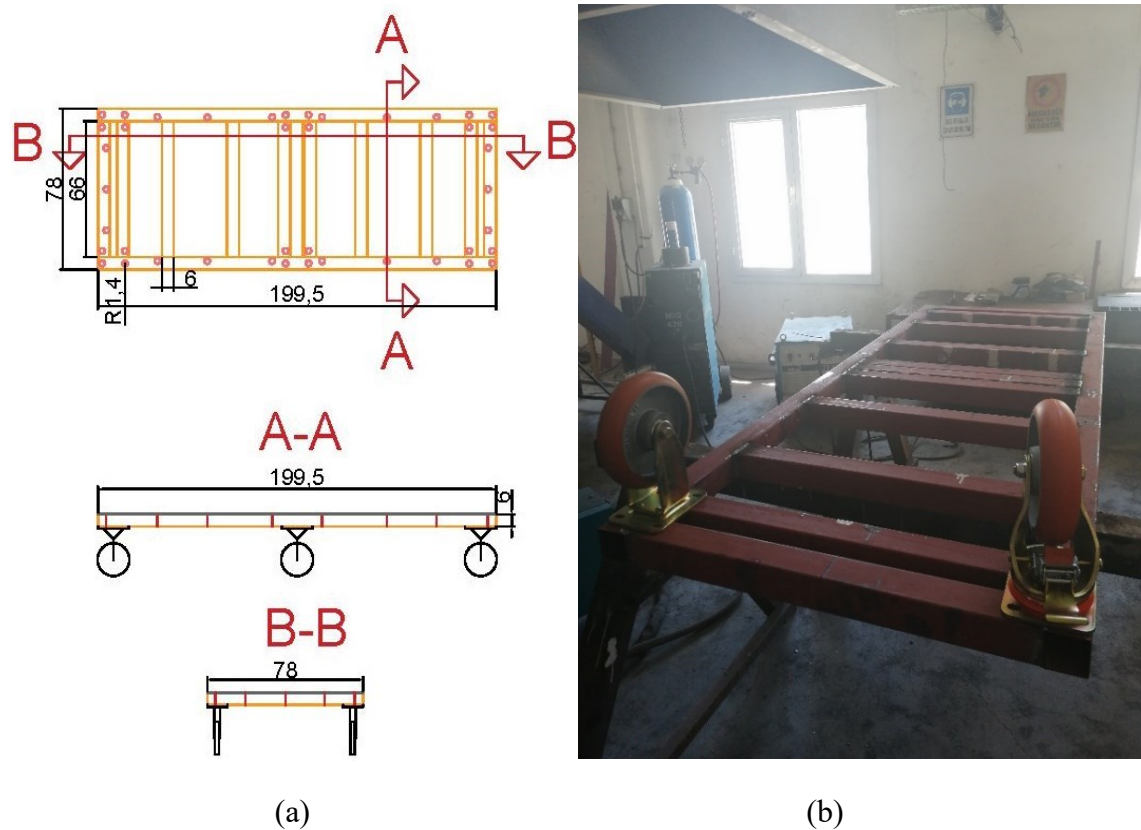


Figure 3.1. (a) Schematic view of the top, side and front of the wheeled platform system, (b) construction of the wheeled platform system in the plant

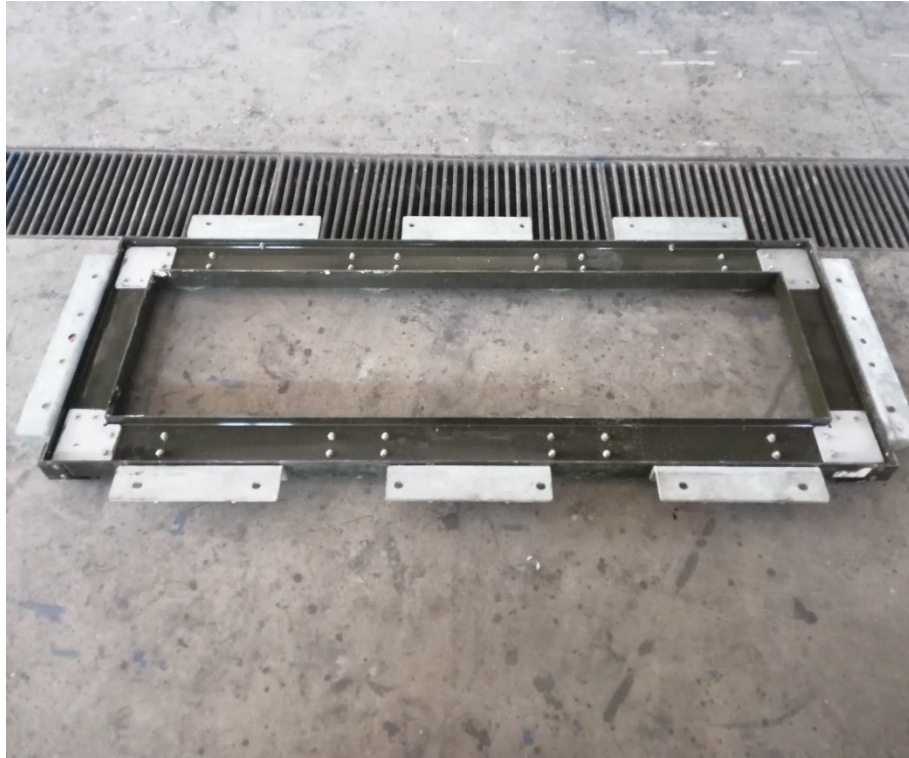


Figure 3.2. Laminar box platform



Figure 3.3. Laminar box (160 cm length, 150 cm depth and 40 cm width)

3.3. Sample Preparation

Silty sand samples have been prepared at the silt content of 5%, 15%, and 35% by weight. Mixtures were prepared for the silty sands experiments in the box as shown in Figure 3.4, 155 cm in length and 77 cm wide. In this box, 50 kilograms of silt and sand samples have been mixed fractionally with shovels for better homogeneity instead of whole samples mixed in one blow.



Figure 3.4. Sample preparation box (155 cm length 77 cm wide)

First tests with a sample of clean sand, then 5%, 15%, and 35% silty sands by weight were performed as loose, medium dense, and dense soil. The mixing process was not performed for clean sand. A mixing process was applied in each experiment with varying silt ratios of clean sand to 5% silty sand, 5% silty sand to 15% silty sand, 15% silty sand to 35% silty sand.

Homogeneous mixtures taken from the sample preparation box were filled into buckets shown in Figure 3.5 (a). As shown in Figure 3.5 (b), the samples put in the buckets have been weighed and filled in the laminar box through the dry filling technique. A hose was

linked to a hopper, and the hose was kept 30 cm away from the soil. Then, the sample filled into the funnel, which fell free into the laminar box. While densification was once not utilized on loose soils, densification was once applied for medium dense and dense soils. A densification plate, as shown in Figure 3.6, was used for the densification process. In the experiments, the laminar box was filled in layers. Densification was applied to the layer in which it was hit twice with a densification plate for medium dense soil at each level. For dense soil, the same process was applied four times.

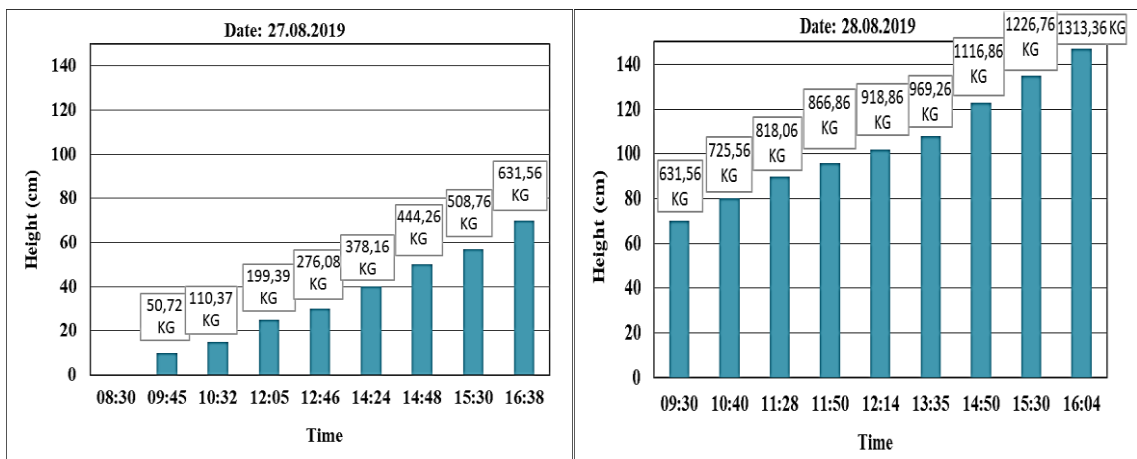


Figure 3.5. (a) Weighed sample (b) Funnel system for the dry filling of the sample

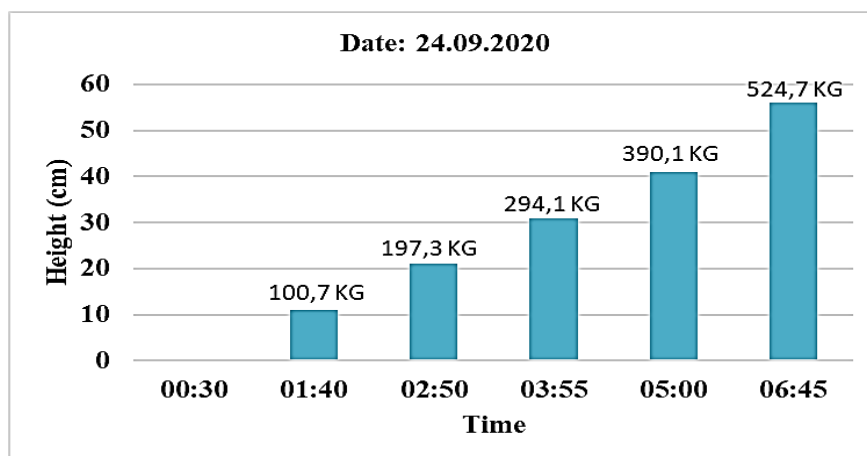


Figure 3.6. Densification plate

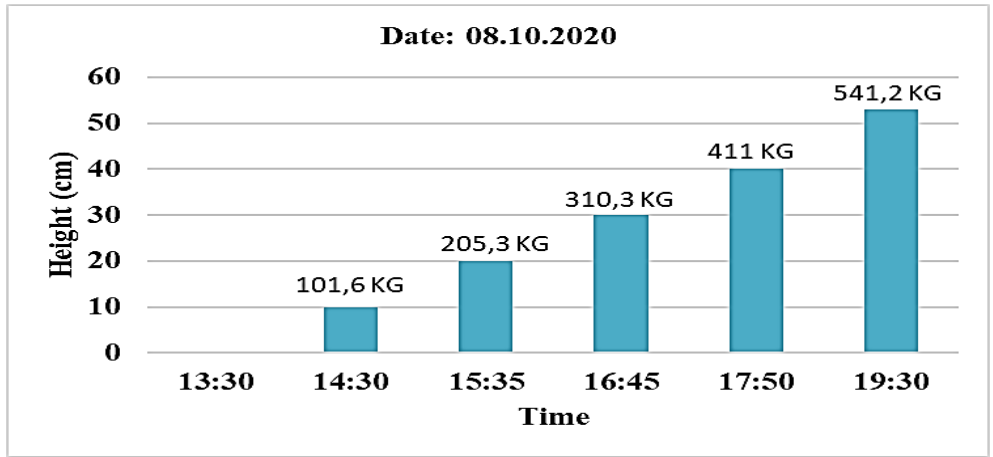
The samples were not filled at once but in layers. The loose soil obtained by the dry filling method on the soils filled with layers was easily transformed into the desired medium-dense and dense soils. Besides, the reason for filling it in layers is to provide a homogeneous relative density throughout the sample. From Figure 3.7 to Figure 3.10, it is shown that the date that each layer was created, the spent time to fill, how high it was filled, and their masses were recorded. For example, in Figure 3.7. (a), for loose clean sand sample preparation, the filling process started at 08.30 on 27.08.2019. The weight of the sample was 50.72 kg, and the height of the sample was 10 cm at 09.45, while at 10.32, it was 110.37 kg of weight and 15 cm of height. On the same date, at 16.38, the filling process was suspended at 631.56 kg and 70 cm height. The filling process, which continued at 09.30 on 28.08.2019, was completed at 16.04 with the weight of 1313.36 kg and the height of 147 cm.



(a)

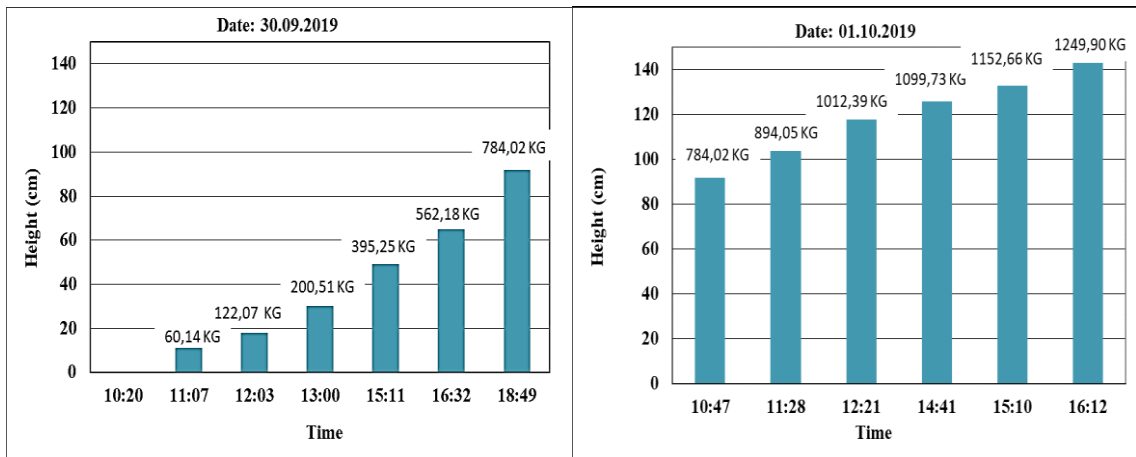


(b)

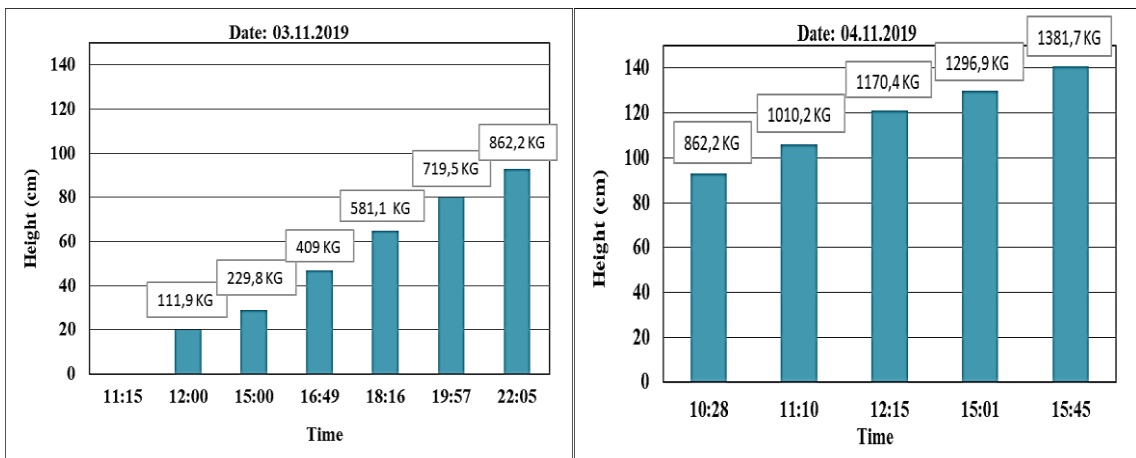


(c)

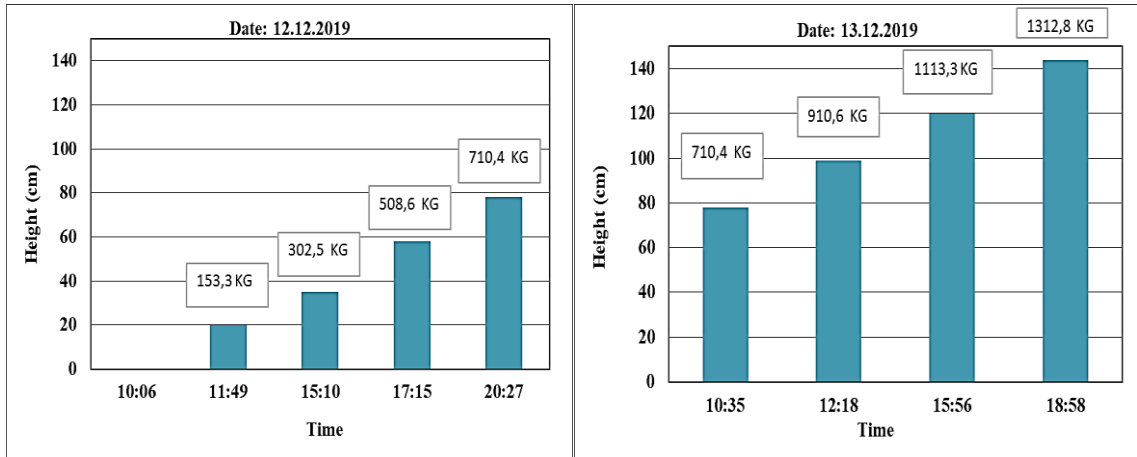
Figure 3.7. Sample preparation process in each layer for (a) loose clean sand (b) medium dense clean sand (c) dense clean sand



(a)

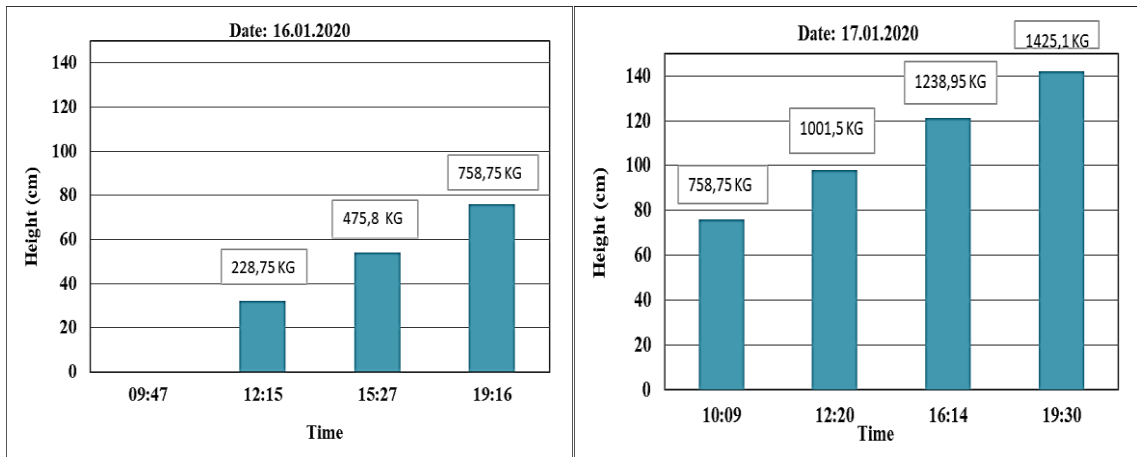


(b)

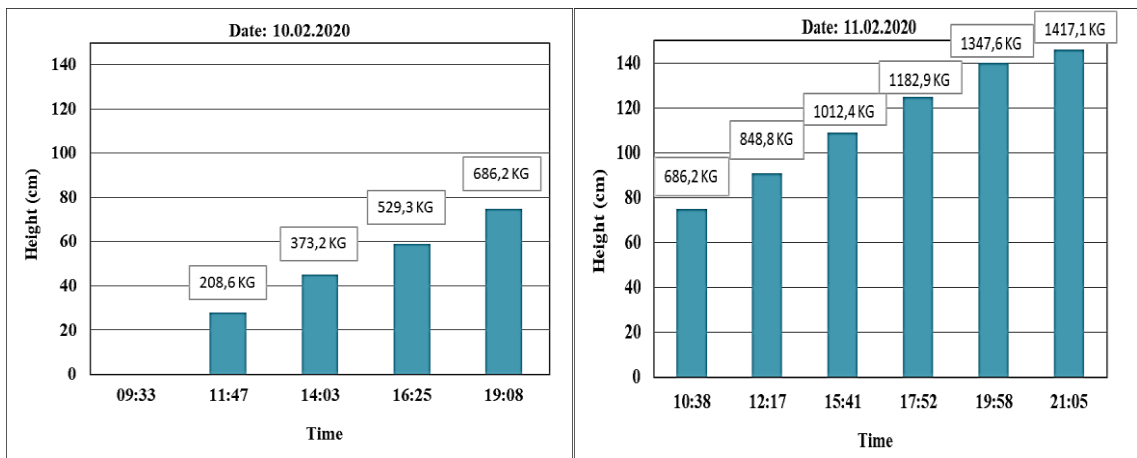


(c)

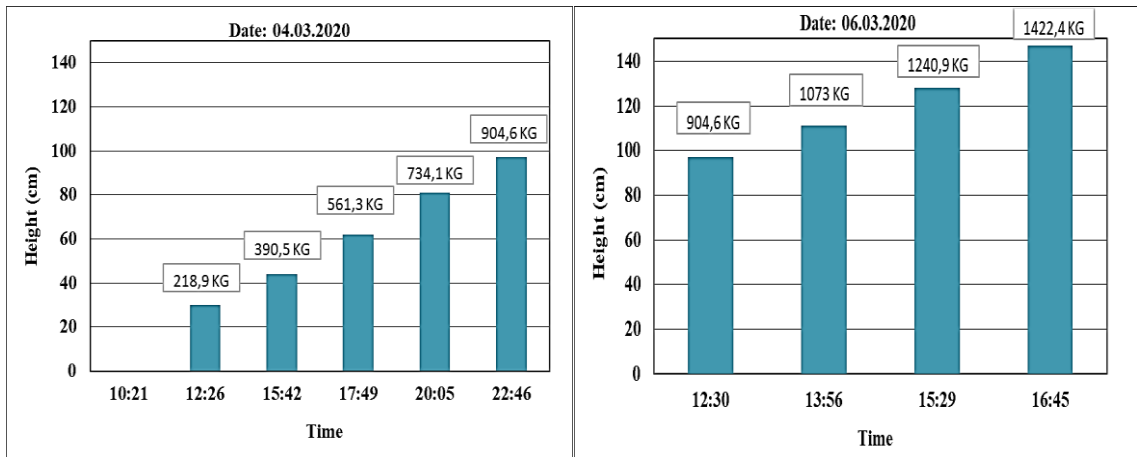
Figure 3.8. Sample preparation process in each layer for 5% silty sands (a) loose (b) dense (c) medium dense



(a)

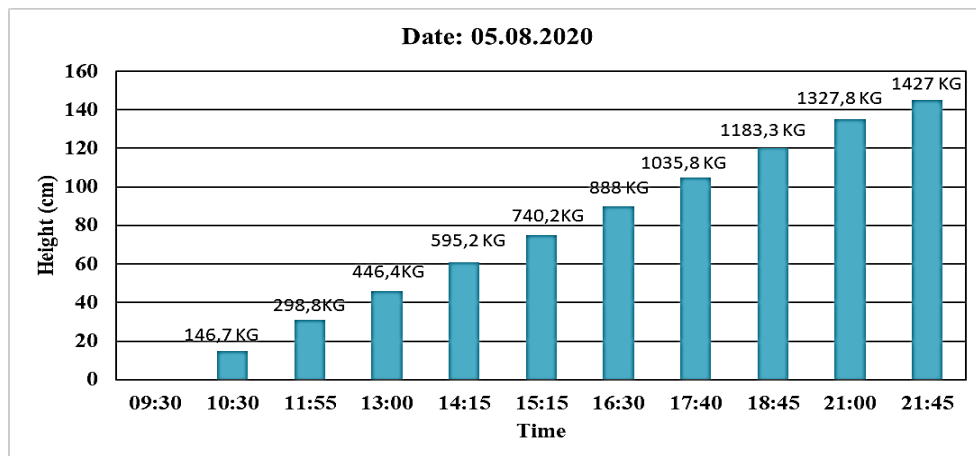


(b)

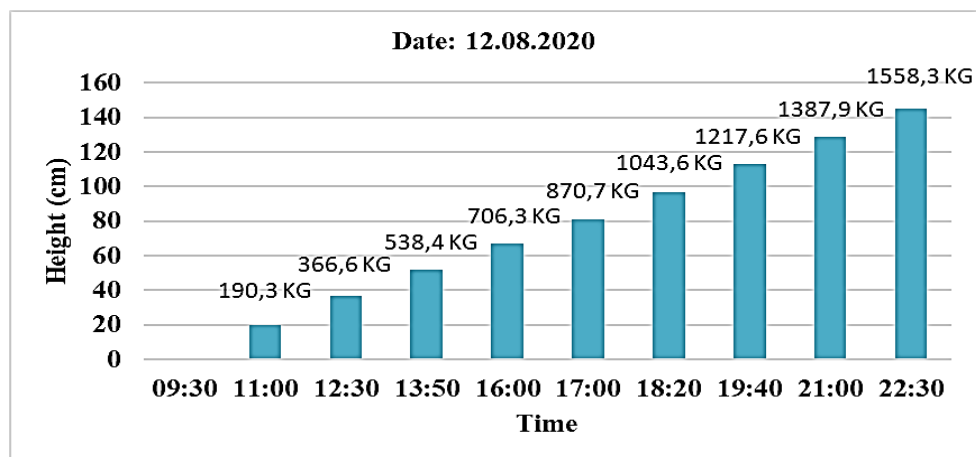


(c)

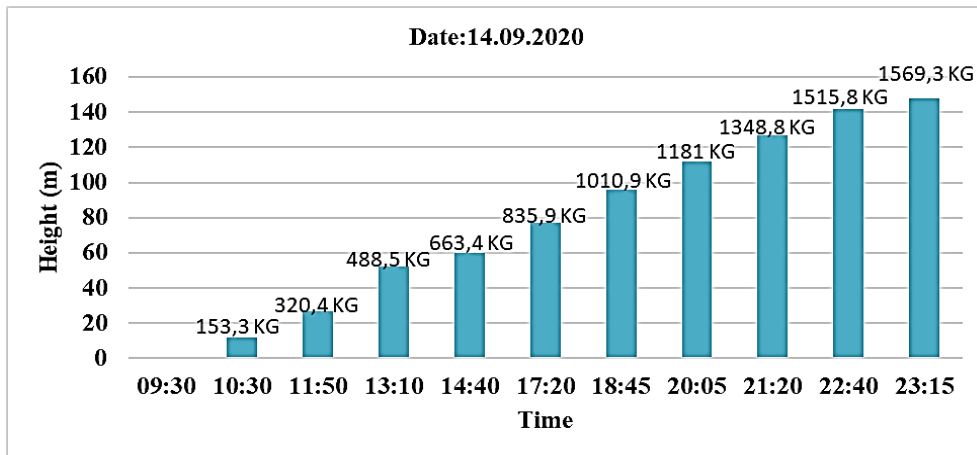
Figure 3.9. Sample preparation process in each layer for 15% silty sands (a) loose (b) medium dense (c) dense



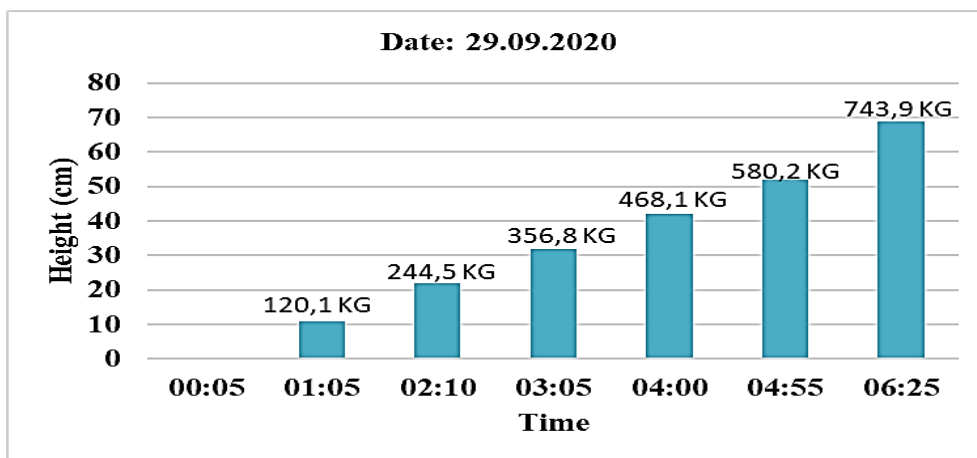
(a)



(b)



(c)



(d)

Figure 3.10. Sample preparation process in each layer for 35% silty sands (a) loose (b) dense (c) medium dense (d) dense

As seen in the graphs above, experiments were spread over time. Since the samples tested were fully saturated with water, the samples were taken from the laminar box after the test were laid in thin layers on the linoleum, as shown in Figure 3.11. The samples could dry for use in the following experiment.



Figure 3.11. The samples laid in thin layers on the linoleum to dry

The dry sample was then saturated with 100% water. First, CO₂ gas was given to the sample for a certain period from the tubes. To fully saturate the sample with water, it is necessary to fill all soil voids with CO₂ gas and then fill them with water. The system was designed to ensure homogeneous distribution of CO₂ gas. In this system, a CO₂ cylinder with a regulator and gas heater is used as the gas source, as shown in Figure 3.12 (a). The regulator was used to regulate gas pressure in CO₂ cylinders, and a gas heater was also used in these regulators to deliver the gas continuously and at the desired pressure. After that, the mechanism placed under the laminar box was prepared. Steel profiles and sheet metal were used for the mechanism. Steel profiles were welded first to form a rectangular mechanism. In a rectangular structure, a steel profile has been added to join the two short sides in the middle. Two holes were drilled for pneumatic hoses connection from the short edge steel profile, as shown in Figure 3.12 (b). Then both sides were welded with sheet metal. A diameter of 0.2 mm was drilled into the sheet metal, as shown in Figure 3.12 (c). In order to prevent the sample from filling the mechanism, a cloth was wrapped around the holes that allow gas to exit since the mechanism was placed at the bottom of the sample. CO₂ gas was released with the hose for passing through the mechanism. Then the CO₂ exiting the holes was released from the bottom of the sample to the entire sample with a homogeneous distribution, as shown in Figure 3.12 (d).

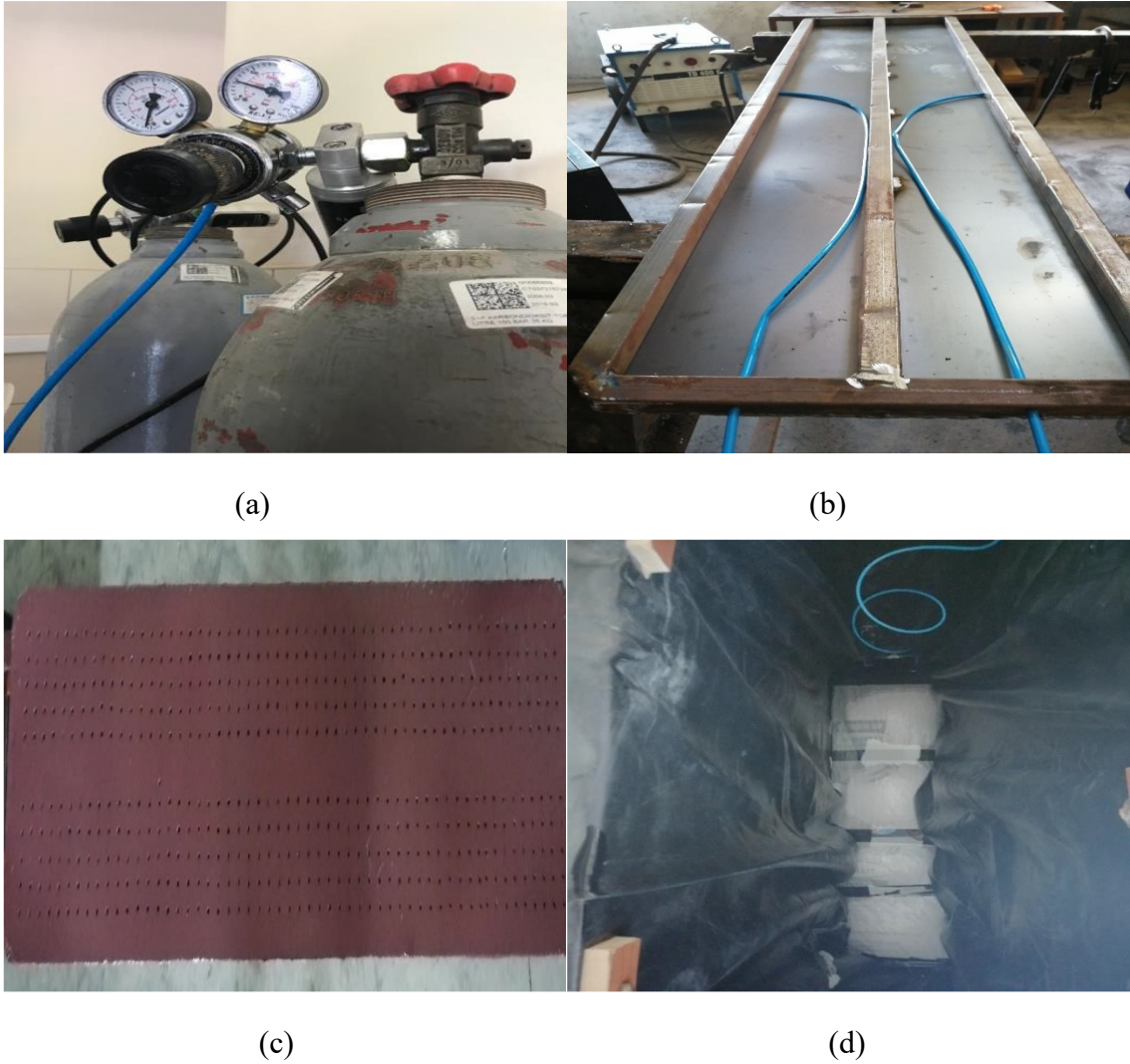


Figure 3.12. (a) CO₂ gas source system (b) pneumatic hoses inserted under the box (c) 2 mm diameter holes for homogeneous distribution (d) CO₂ gas delivery mechanism to the sample

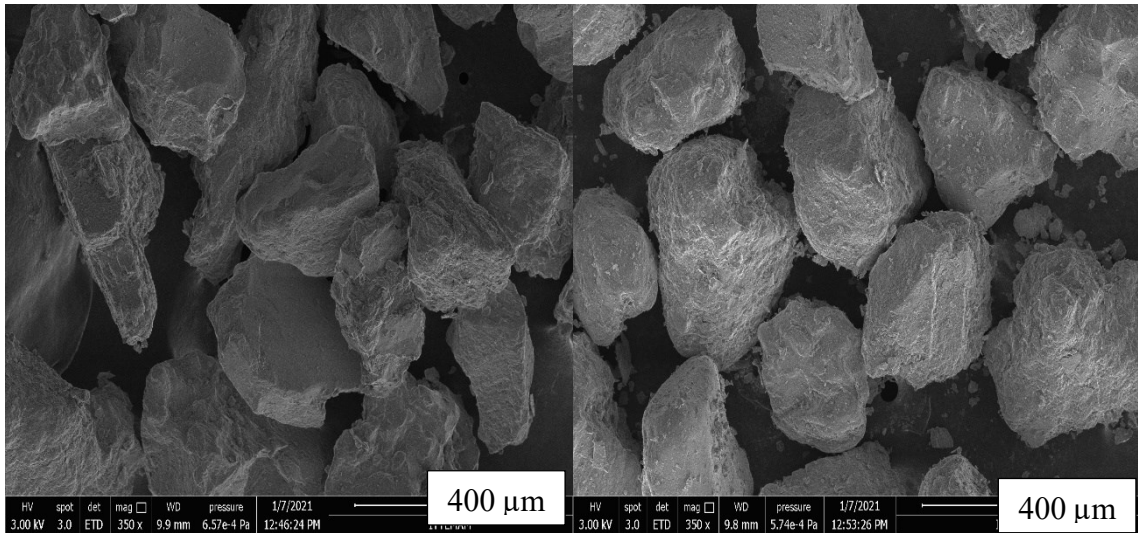
CO₂ gas was given with 0.2 bar pressure in all experiments. CO₂ gas releasing times are given in the Table 3.1. for each experiment and vary between 24 hours and 1 hour. Due to the difference in density and silt percentages of the sample, CO₂ gas was applied at different times in each experiment. It has been observed that the CO₂ gas given for 1 hour is sufficient to saturate the sample with water fully.

Table 3.1. CO₂ gas pressure and CO₂ gas application given in experiments.

Experiment	Gas pressure (bar)	Application of Gas given (hour)
T1 - clean sand	0.2	24
T2 - clean sand	0.2	1
T3 - clean sand	0.2	1
T4 - 5% silty sands	0.2	24
T5 - 5% silty sands	0.2	2
T6 - 5% silty sands	0.2	1
T7 - 15% silty sands	0.2	1
T8 - 15% silty sands	0.2	1
T9 - 15% silty sands	0.2	1
T10 - 35% silty sands	0.2	1
T11 - 35% silty sands	0.2	1
T12 - 35% silty sands	0.2	1
T13 - 35% silty sands	0.2	1

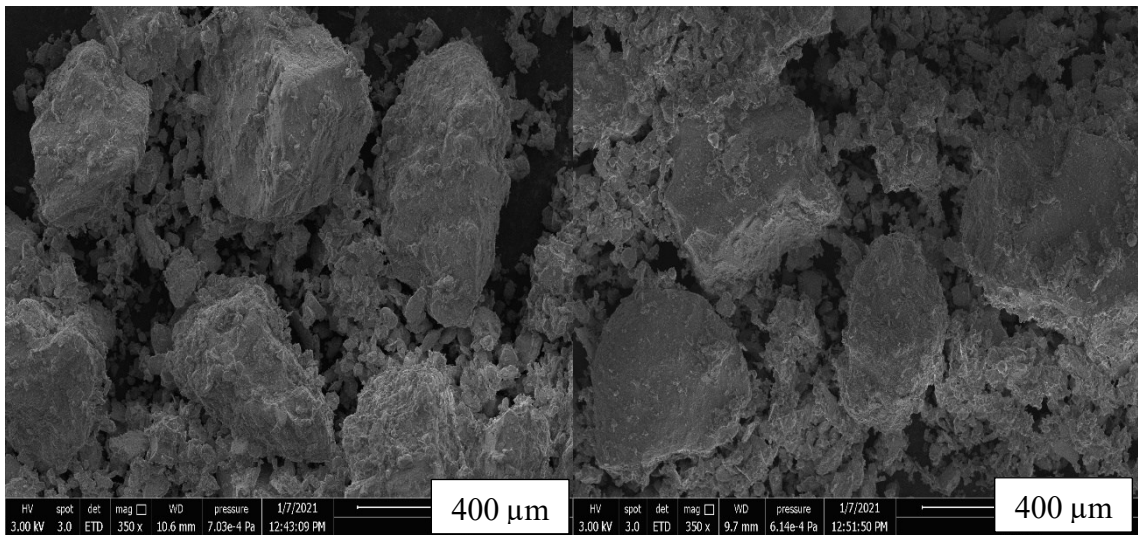
After dry filling and CO₂ degassing, the flow rate was measured, and the quenching process was started with a hose to saturate the sample with water fully. While it takes less time to saturate the sand with water, this period extends to a few days as the silt ratio increases in the silty sand mixture. The total liters of water delivered in each experiment were recorded to calculate the water content.

In Figure 3.13 (a), (b), (c), and (d), scanning electron microscope (SEM) analysis images of clean sand, 5%, 15% and 35% silty sand samples at 400 μm resolution are given, respectively. This analysis was done at IZTECH Center for Materials Research. As the silt ratio increases, the internal force between the sands decreases. Inter-grain contacts are dominant in 5% and 15% silty sands, while inter-fine contacts are dominant in 35% silty sands.



(a)

(b)



(c)

(d)

Figure 3.13. SEM view of (a) clean sand (b) 5% silty sand (c) 15% silty sand (d) 35% silty sand samples at 400 μm resolution

3.4. Properties of Sample

For all samples, maximum void ratio (e_{max}), minimum void ratio (e_{min}), specific gravity (G_s) data were obtained from Saritaş (2021), as shown in Table 3.2.

Table 3.2. Physical properties of sand and silty sands (Saritas, 2021)

Soil Type	FC	G_s	e_{max}	e_{min}
-	%	-	-	-
Clean Sand	0	2,64	1	0,72
Silty Sand	5	2,64	0,94	0,68
Silty Sand	15	2,65	0,88	0,58
Silty Sand	35	2,66	0,83	0,43

Void ratio (e) and relative density (D_r) were calculated using Table 3.2.

Void ratio (e) is calculated by Equation 3.1.

$$S * e = w * G_s \quad (3.1)$$

where S is the degree of saturation and w is the water content. The degree of saturation of the sample is taken as 1 because the sample is fully saturated with water. Thus, Equation 3.1 has turned into Equation 3.2.

$$e = w * G_s \quad (3.2)$$

Relative density (D_r) is calculated by Equation 3.3.

$$D_r = \frac{e_{max} - e}{e_{max} - e_{min}} \quad (3.3)$$

The laminar box consists of 160 cm length, 40 cm width and 150 cm depth, as mentioned before. Since the samples are filled from bottom to top, the total volume depends only on the height of the filled sample. Each sample was filled at different heights close to the height of the laminar box.

Total volumes are calculated by Equation 3.4.

$$Total\ Volume = Box\ Length * Box\ Width * Depth\ of\ The\ Sample \quad (3.4)$$

Water content is calculated by Equation 3.5.

$$\text{Water Content} = \frac{\text{Weight of Water}}{\text{Weight of Solid}} \quad (3.5)$$

Density is calculated by Equation 3.6.

$$\text{Density} = \frac{\text{Weight of Solid} + \text{Weight of Water}}{\text{Total Volume}} \quad (3.6)$$

Tables from 3.3 to 3.6 show the weight of solid, water weight, total volume, water content, density, void ratio (e) and relative density (D_r) for 13 experiments performed.

Table 3.3. For the clean sand samples prepared, the weight of the solid, water weight, calculated total volume, water content, density, void ratio (e) and relative density (D_r)

Test No.	FC	Weight of solid	Weight of water	Total Volume	Water content	Density	e	D_r
-	%	kg	kg	m ³	-	kg/m ³	-	%
T1	0	1313,4	473,1	0,941	0,36	1899	0,95	18
T2	0	524,7	168,2	0,358	0,32	1933	0,85	55
T3	0	541,2	157,2	0,339	0,29	2059	0,77	83

Table 3.4. For the 5% silty sand samples prepared, the weight of the solid, water weight, calculated total volume, water content, density, void ratio (e) and relative density (D_r)

Test No.	FC	Weight of solid	Weight of water	Total Volume	Water content	Density	e	D_r
-	%	kg	kg	m ³	-	kg/m ³	-	%
T4	5	1249,9	423,2	0,915	0,34	1828	0,89	18
T5	5	1381,7	387,0	0,902	0,28	1960	0,74	77
T6	5	1312,8	428,0	0,922	0,33	1889	0,86	31

Table 3.5. For the 15% silty sand samples prepared, the weight of the solid, water weight, calculated total volume, water content, density, void ratio (e) and relative density (D_r)

Test No.	FC	Weight of solid	Weight of water	Total Volume	Water content	Density	e	D_r
-	%	kg	kg	m ³	-	kg/m ³	-	%
T7	15	1425,1	440,1	0,909	0,31	2052	0,82	21
T8	15	1417,1	409,3	0,934	0,29	1955	0,77	38
T9	15	1422,4	397,8	0,941	0,28	1935	0,74	46

Table 3.6. For the 35% silty sand samples prepared, the weight of the solid, water weight, calculated total volume, water content, density, void ratio (e) and relative density (D_r)

Test No.	FC	Weight of solid	Weight of water	Total Volume	Water content	Density	e	D_r
-	%	kg	kg	m^3	-	kg/m^3	-	%
T10	35	1427,0	376,2	0,928	0,26	1943	0,70	32
T11	35	1558,3	374,9	0,928	0,24	2083	0,64	48
T12	35	1569,3	435,9	0,909	0,28	2206	0,74	23
T13	35	743,9	143,7	0,442	0,19	2010	0,51	79

3.5. Conclusion

A fixed wall laminar box was prepared for laboratory experiments. A wheeled platform system was set up to move the laminar box in the laboratory. After the laminar box was fixed, samples were started to be prepared for each experiment. A homogeneous mixture was obtained with the sample preparation box for silty sand mixtures. Samples were densified with a densification plate for medium dense and dense samples. The loose soil obtained by the dry fill method in soils filled with layers was easily transformed into the desired medium dense and dense soils. The samples were filled layer by layer to obtain a homogeneous relative density in all samples. All pores were filled with carbon dioxide gas before quenching to saturate the samples fully. During the preparation, the weight of the solid and the water weight of the samples were measured and recorded. Total volume, water content, density and void ratio were calculated. Relative density was calculated using physical properties e_{max} , e_{min} and G_s (Saritas, 2021). The following Chapter presents laboratory tests.

CHAPTER 4

LABORATORY TESTS

4.1. Introduction

The experiments in this study aimed to examine the effect of fines content on CPT resistance in silty sands. Laboratory experiments are well organized and created with precise work to provide data. Although it is a disadvantage that laboratory experiments are less representative of the sample and disturbed, it has the advantage of being controlled and well defined.

Experiments performed on laminar box 150 cm depth, 40 cm wide, 160 cm length, and test systems are shown schematically in Figure 4.1. A total of 13 tests were carried out on clean sand and 5%, 15% and 35% silty sand. Tests were prepared for each of the clean sand and 5%, 15% and 35% silty sands as loose, medium-dense and dense. The locations of the experiments are given in the Figure. Accordingly, 40 cm longitudinally from the left side, 20 cm wide piezocone penetration test (CPTu) from both sides, 40 cm longitudinally and 20 cm wide seismic cone penetration test (SCPT) from both sides, 80 cm from both sides, 20 cm wide direct push permeability test (DPPT) was performed in the given areas.

This section explains the piezocone penetration test (CPTu), seismic cone penetration test (SCPT) and direct push permeability test (DPPT). It then provides descriptions of the equipment, test procedures, test standards and measured data from tests.

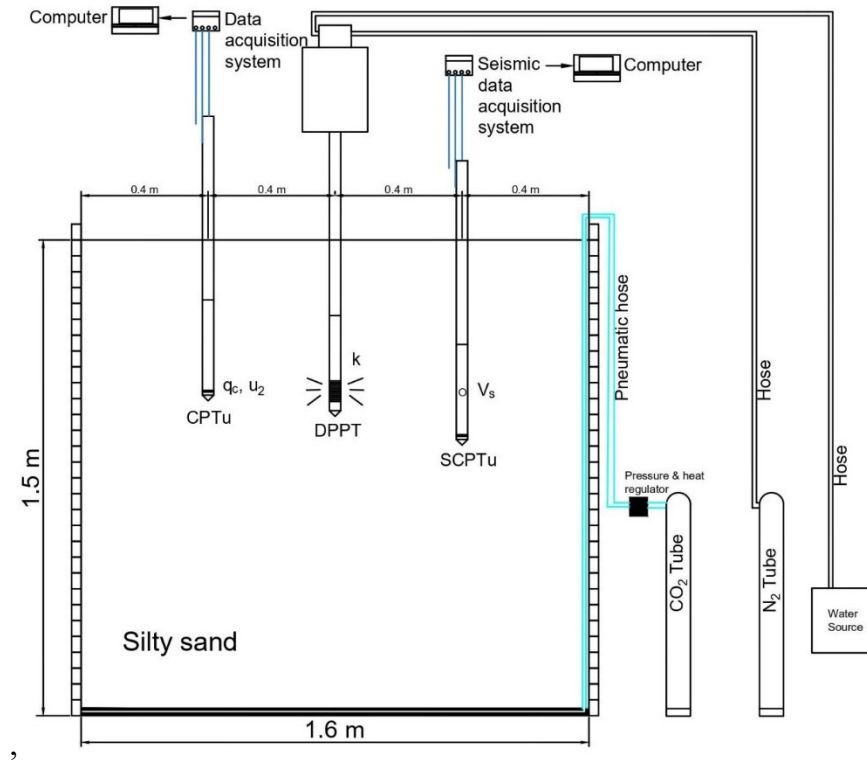


Figure 4.1. Locations of CPTu, SCPT, DPPT tests in the box

4.2. Piezocone Penetration Test (CPTu)

First, CPTu tests were performed on a box for obtaining soil parameters. CPTu is defined as a cone that is driven into the ground at a constant velocity at the end of a series of rods, and continuous or periodic measurements of the cone's penetration resistance are made. With the CPTu test, pore water pressure can also be measured besides cone penetration resistance and sleeve resistance.

CPTu testing has some advantages: fast and continuous profiling, cost-effective and functional equipment, and reliable and repeatable operator-independent results.

4.2.1. Historical Development of CPTu

The developed electric piezocone was first used in 1974 by Janbu and Senneset to measure pore water pressure. Wissa et al. in the USA (1975), a similar study was performed almost simultaneously, and a piezometer probe was developed to measure pore

water pressure when paused during penetration, as shown in Figure 4.2 (a). In the following years, the Wissa type piezometer probe with a 60-degree cone and different filter positions was introduced by Schmertmann (1978) and Baligh et al. (1980) for various studies. However, only pore water pressure could be measured in these studies, and separate tests were performed for CPTu data. Pore water pressure and cone tip resistance were combined in a study by Roy et al. in 1980. on the same probe. The filter element position has been diversified as U_1 , U_2 and U_3 in the studies, as shown in Figure 4.2 (b). It is the most widely used U_2 location today.

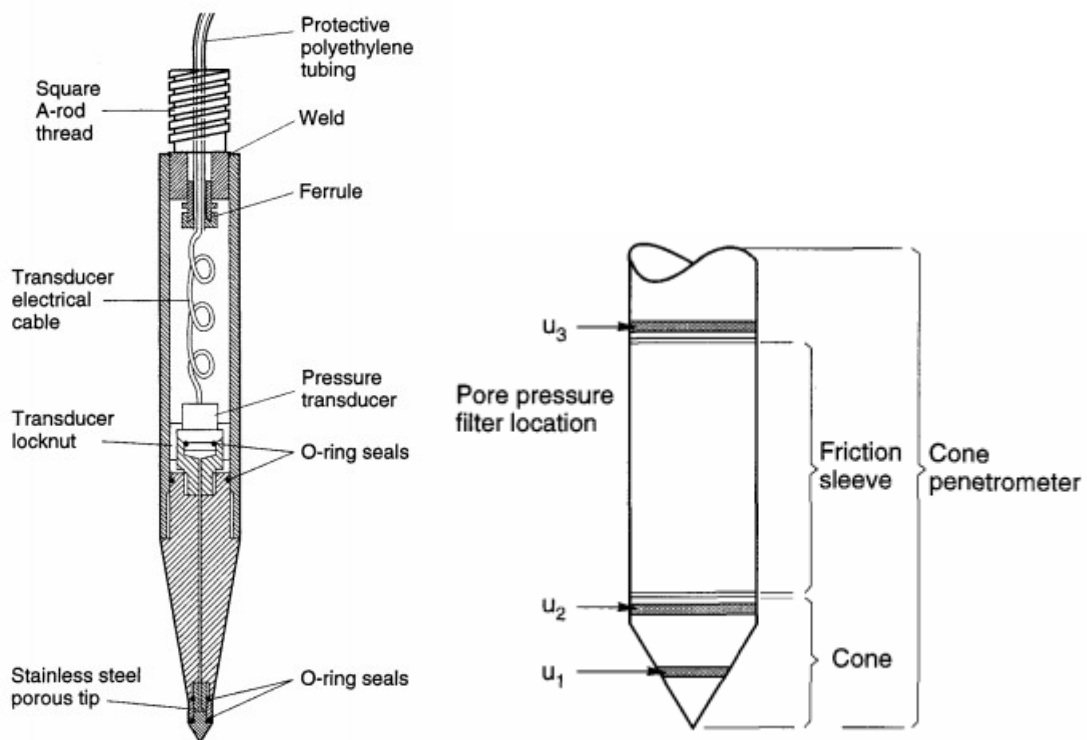


Figure 4.2. (a) The Wissa piezometer probe (b) filter element position

(Source: CPT in Geotechnical Practice Lunne, 1997)

4.2.2. Test Equipment

CPTu equipment consists of 3 parts. A hydraulic pushing system, a data acquisition system and a probe with a cable adapter were used for the CPTu. The data acquisition system and probe with cable adapter are from Geotech Co., Sweden. The probe consists

of piezecone and nova, as shown in Figure 4.3. (a). A conical tip with an angle of 60 degrees and a base area of 10 cm^2 was used in the piezocone. Filter element position was used as U_2 . Figure 4.3. (b) shows a 57 cm length probe and 81 cm length rod. The cable adapter was connected to the nova and data transfer was performed over the connected cable. In addition, CPTu tests were performed by adding a rod up to 1.2 meters to the probe.

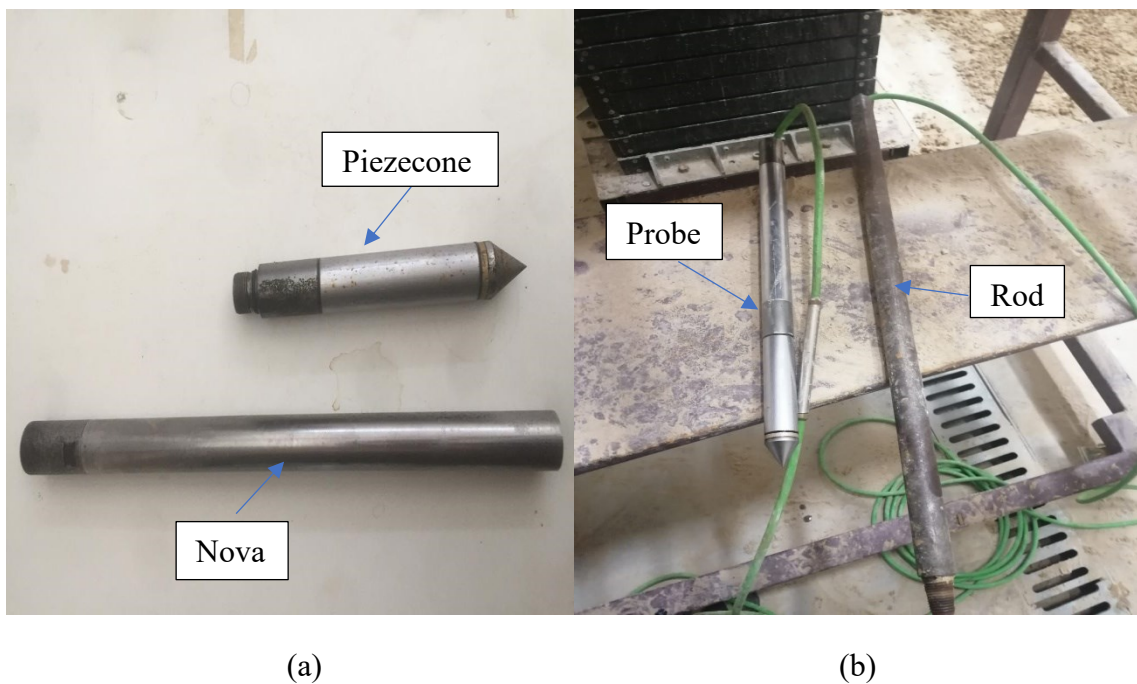


Figure 4.3. (a) Piezocone and Nova (b) Probe with a cable adapter and Rod

Data acquisition system (DAQ) consists of depth encoder, probe with cable adapter, interface, and computer. Signals from the depth encoder and the probe's sensor data are taken to the interface and processed there, then output to the computer as shown in Figure 4.4 (a). The interface box used in the experiment is shown in Figure 4.4 (b).

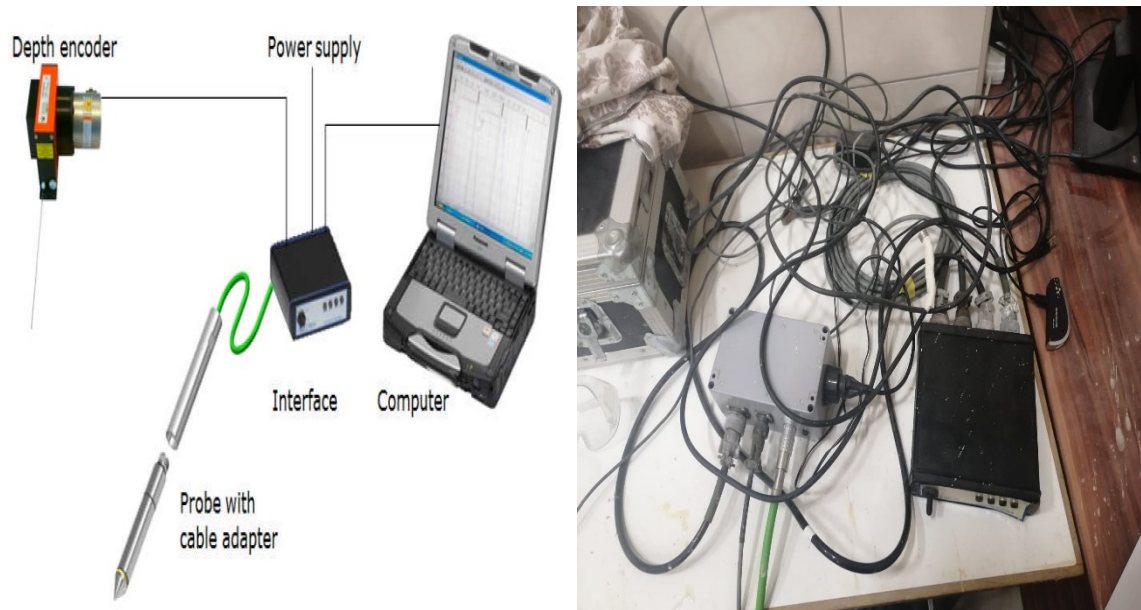


Figure 4.4. (a) Data acquisition system (b) Interface Box

(Source: CPT Geotech NOVA MANUAL, 2015)

As shown in Figure 4.5, a hydraulic pushing system was used to push the probe and rod soil. The samples penetrated the soil up to about 1.2 meters with a hydraulic platform at penetration rates ranging from 0.8 to 1.5 cm/sec.

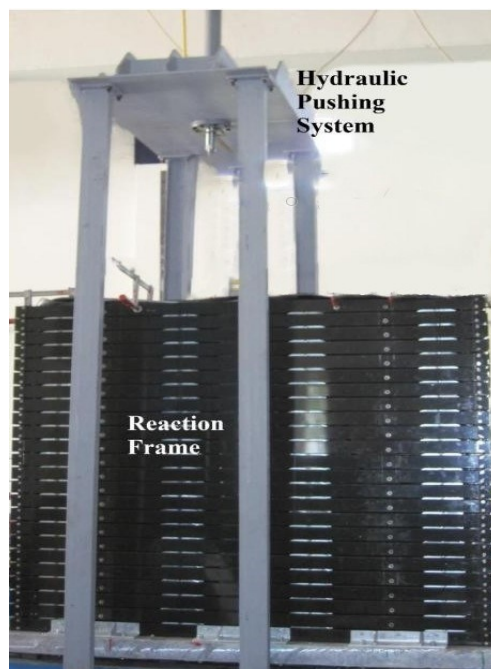


Figure 4.5. Hydraulic pushing system

4.2.3. Test Procedure

These experiments were carried out following the ASTM D5778-20 Standard Test Method for Electronic Friction Cone and Piezocone Penetration Testing of Soils and ASTM D6067/D6067M-17 Standard Practice for Using the Electronic Piezocone Penetrometer Tests for Environmental Site Characterization and Estimation of Hydraulic Conductivity.

Geotech Firm's software was used for the CPTu experiments of the samples. Before the experiment, after the hydraulic pushing system was set to CPTu position and fixed, it was connected to the depth encoder, and zero tests were performed. As a team using software, a hydraulic pushing system, and probe penetration, experiments were started simultaneously. Experiments were carried out continuously up to about 1.2 meters. CPTu test performed in the laboratory given in Figure 4.6.

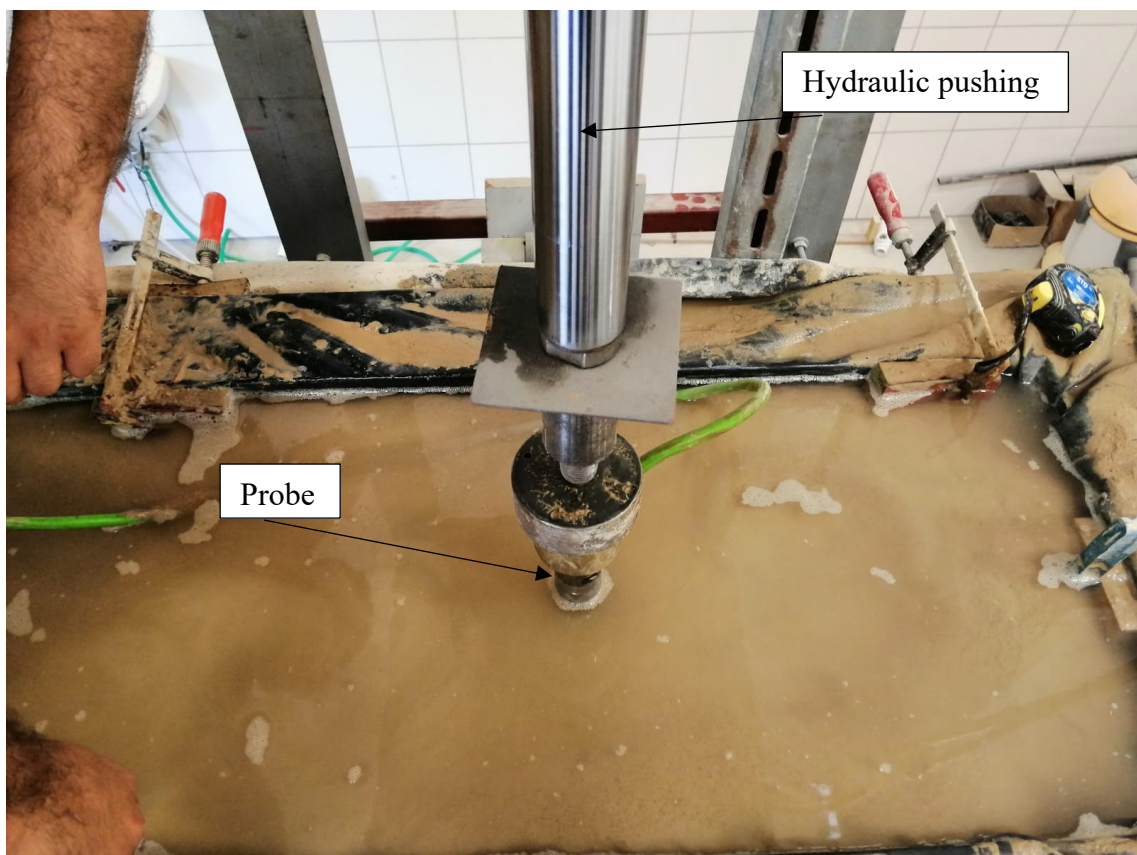


Figure 4.6. The CPTu experiment performed in the laboratory

4.2.4. CPTu Test Data

Figure 4.7 - Figure 4.10 shows the cone resistance and pore water pressure data of clean sand and 5%, 15% and 35% silty sand, respectively, together with the penetration depth.

D_r is between 15 - 22 for Test 1, between 35 - 50 for Test 2 and between 45 - 65 for Test 3 in clean sand. In Figure 4.7. (a), The cone resistance given throughout the depth is around 0.25 MPa in Test 1, 1.3 MPa in Test 2 and 1.9 MPa in Test 3. In Figure 4.7. (b), the pore water pressure given throughout the depth is around 14 kPa in Test 1, 6 kPa in Test 2 and 4.5 kPa in Test 3.

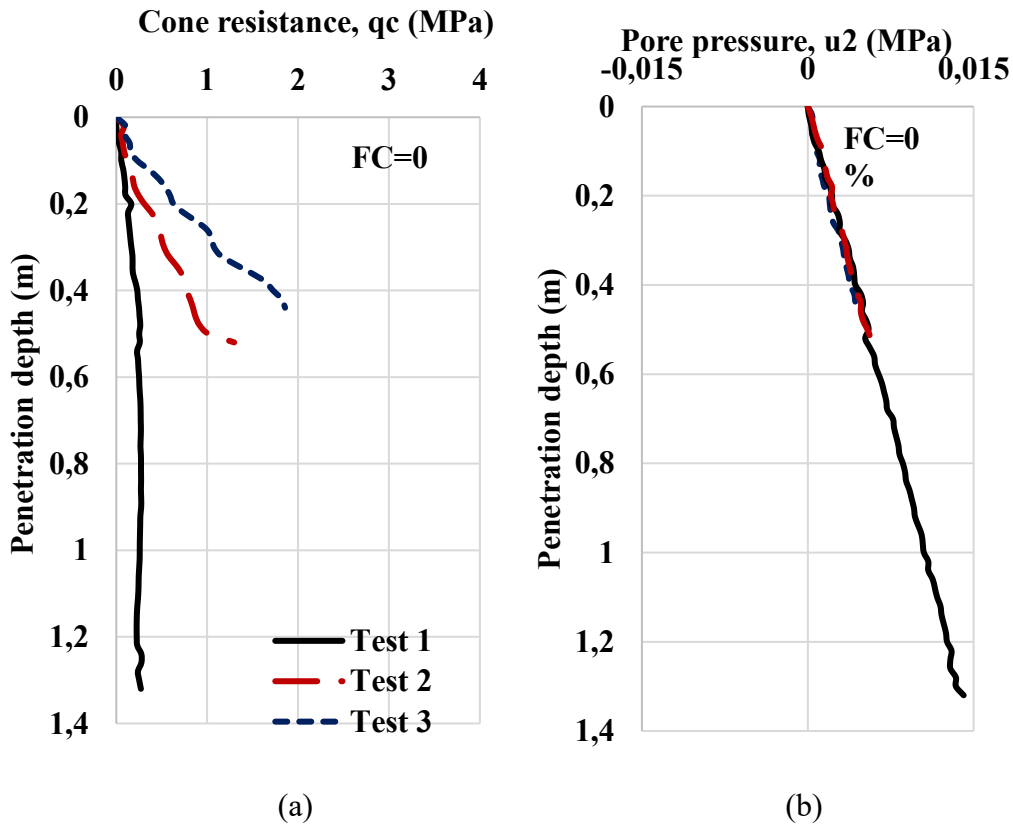


Figure 4.7. (a) The cone resistance (b) pore water pressure data of clean sand with the penetration depth for Test 1, Test 2 and Test 3

D_r is 18 for Test 4, between 23-25 for Test 6 and between 70 - 75 for Test 5 in 5% silty sands. In Figure 4.8. (a), the cone resistance given throughout the depth is around 0.15 MPa in Test 4, 0.7 MPa in Test 6 and 2.8 MPa in Test 5. In Figure 4.8. (b), the pore water pressure given throughout the depth is around 13.6 kPa in Test 4, 13 kPa in Test 6 and 7.8 kPa in Test 5.

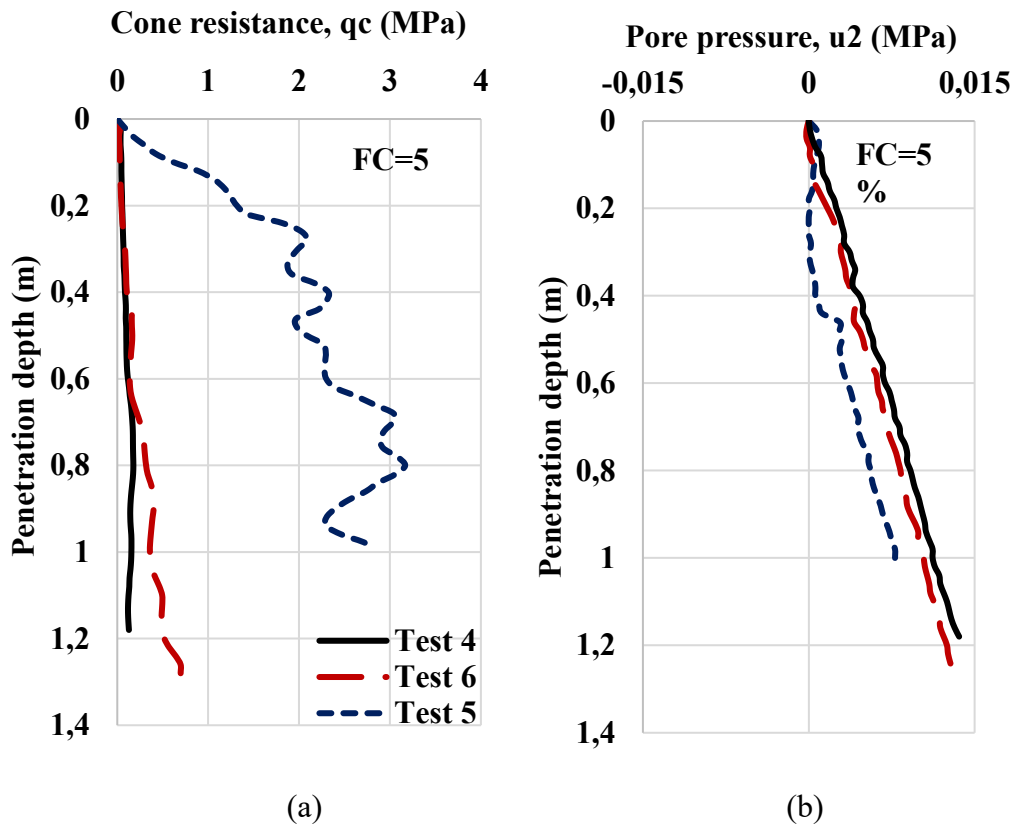


Figure 4.8. (a) the cone resistance (b) pore water pressure data of 5% silty sand with the penetration depth for Test 4, Test 5 and Test 6

In 15% silty sands, D_r is between 21 – 23 for Test 7, between 35-40 for Test 8, and between 35-44 for Test 9. In Figure 4.9. (a), the cone resistance given throughout the depth is around 0.13 MPa in Test 7, 0.6 MPa in Test 8 and 0.6 MPa in Test 9. In Figure 4.9. (b), the pore water pressure given throughout the depth is around 14.5 kPa in Test 7, 13.6 kPa in Test 8 and 14.4 kPa in Test 9.

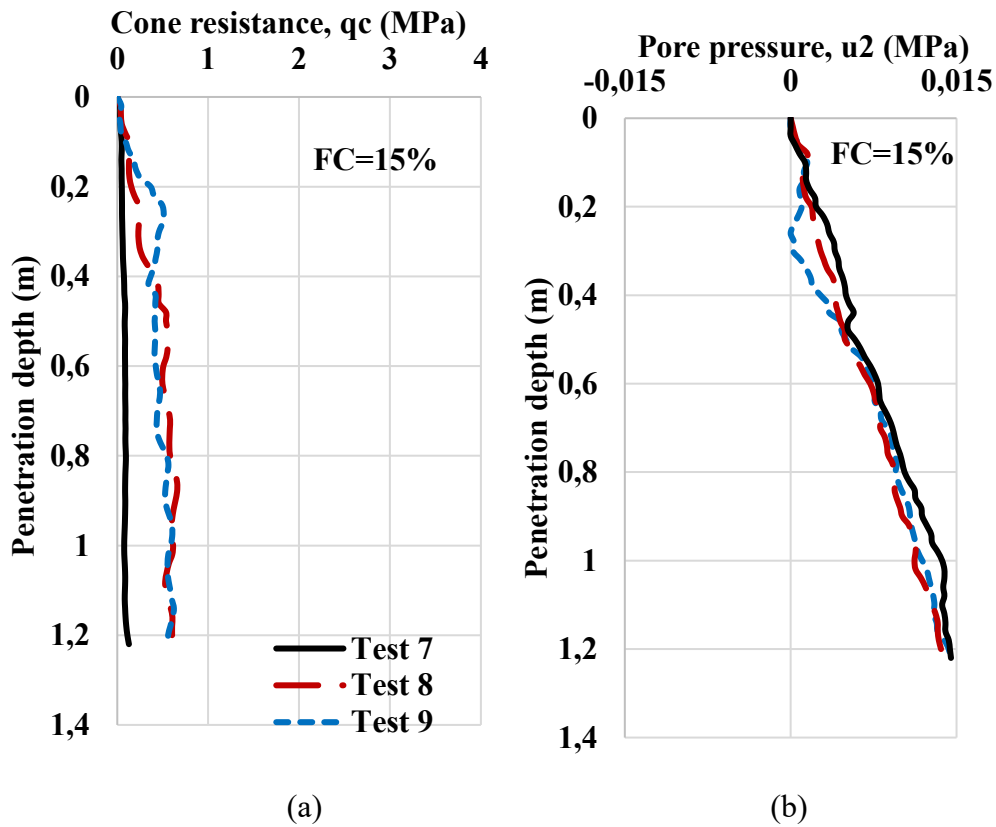


Figure 4.9. (a) the cone resistance (b) pore water pressure data of 15% silty sand with the penetration depth for Test 7, Test 8, and Test 9

In 35% silty sands, D_r is between 35-36 for Test 10, between 34 – 46 for Test 12, and between 30 - 55 for Test 11. In Figure 4.10. (a), the cone resistance given throughout the depth is varying 0.25 – 0.47 MPa in Test 10, 0.27 - 0.51 MPa in Test 12, and 0.27 – 0.81 MPa in Test 11. In Figure 4.10. (b), the pore water pressure given throughout the depth is around 2.5 kPa in Test 10, 15 kPa in Test 12, and 15 kPa in Test 11. In Test 11 and Test 12, negative pore water pressure occurs, which indicates the expansion behavior of the soil during penetration.

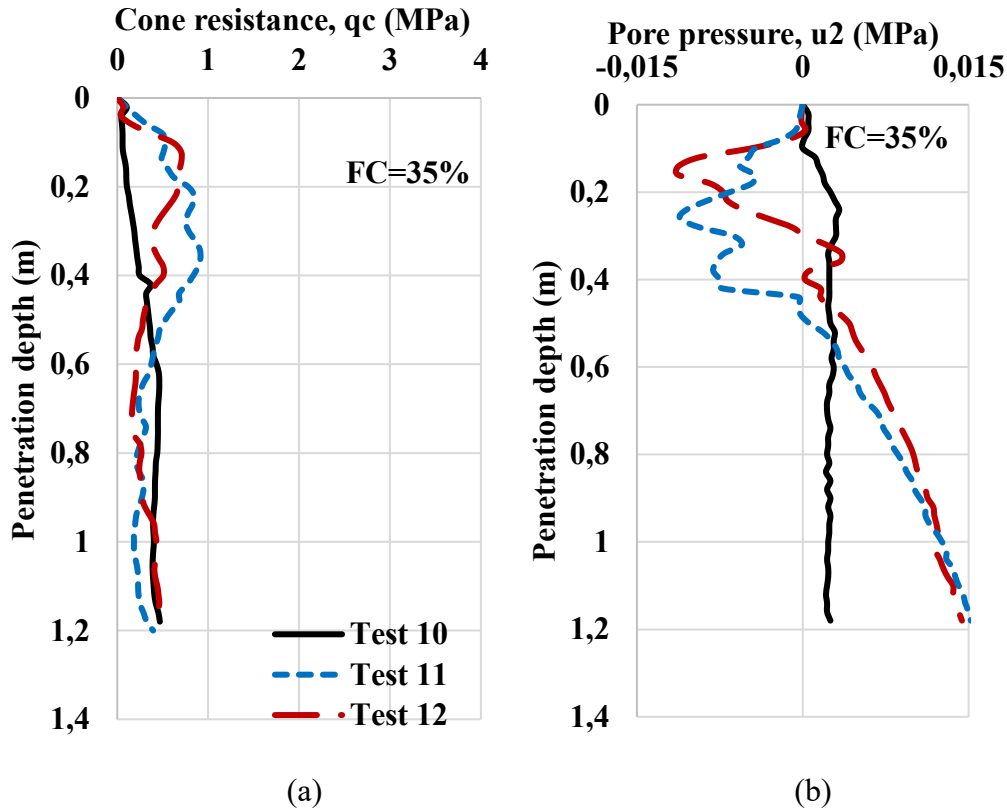


Figure 4.10. (a) the cone resistance (b) pore water pressure data of 35% silty sand with the penetration depth for Test 10, Test 11 and Test 12

In general, cone resistance increases as the relative density increases in the sand and silty sands. Also, cone resistance decreases as the silt ratio increases. Generally, in the sand and silty sands, the lower the relative density, the higher the pore water pressure is. Also, the higher the silt ratio, the higher the pore water pressure is. Negative pore water pressure occurred in medium and dense 35% silty sands. High normal stresses dominate the pore water pressure measured near the tip of the cone, while high shear stresses dominate the pore water pressure in the cylindrical shaft (U_2 location). Increment in the shear stresses can cause negative pore water pressure in medium dense and dense silty sands (Lunne, 1997).

4.3. Seismic Cone Penetration Test (SCPT)

Used to measure seismic waves, SCPT appears to be a reliable test for predicting geotechnical parameters. SCPT is made by adding a few pieces of equipment to CPT equipment. Seismometer within the probe measures seismic waves, compression (P) and shear (S) waves. The S plate was used to calculate the shear wave velocity in the experiment. In this study, SCPT was performed to find the shear modulus with shear wave velocity, which is one of the intermediate steps to calculate the volume compressibility coefficient and coefficient of consolidation.

4.3.1. Test Equipment

SCPT equipment was purchased from Geotech company. SCPT equipment was easily created by adding a steel plate, sledgehammer, and seismic data acquisition system to CPTu equipment a hydraulic pushing system, a data acquisition system, and a probe with a cable adapter. Experiments were created by a sledgehammer with the triggered cable connection to hit the left steel plate with the crocodile clamped cable connection to find only the left polarized shear wave. The velocity seismometer attached to the CPT probe, 1.7 cm in diameter and positioned horizontally at a frequency of 28 Hz, detects the horizontal component of the incoming shear wave and is sent to the seismic data collection box with a seismic cable, as shown in Figure 4.11. The sledgehammer, steel plate and data collection box used in the experiment are shown in Figure 4.12.

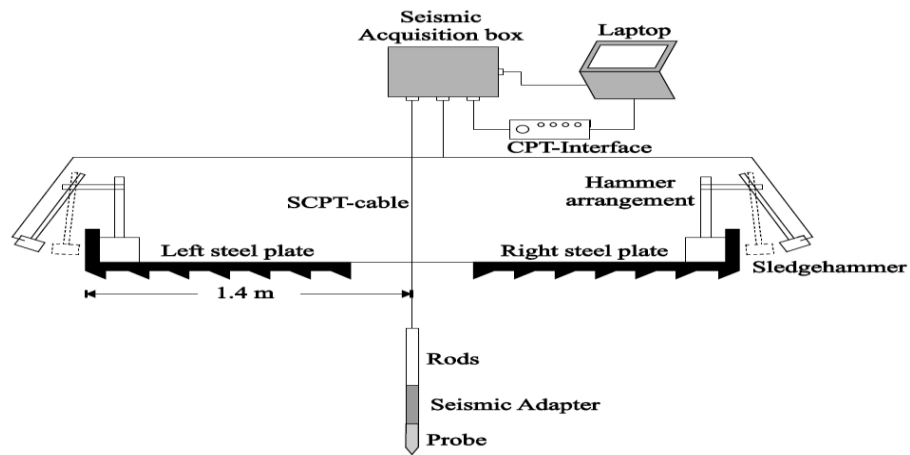


Figure 4.11. SCPT data acquisition system

(Source: Holmsgaard et al. Interpretation of Seismic Cone Penetration Testing in Silty Soil, 2016)

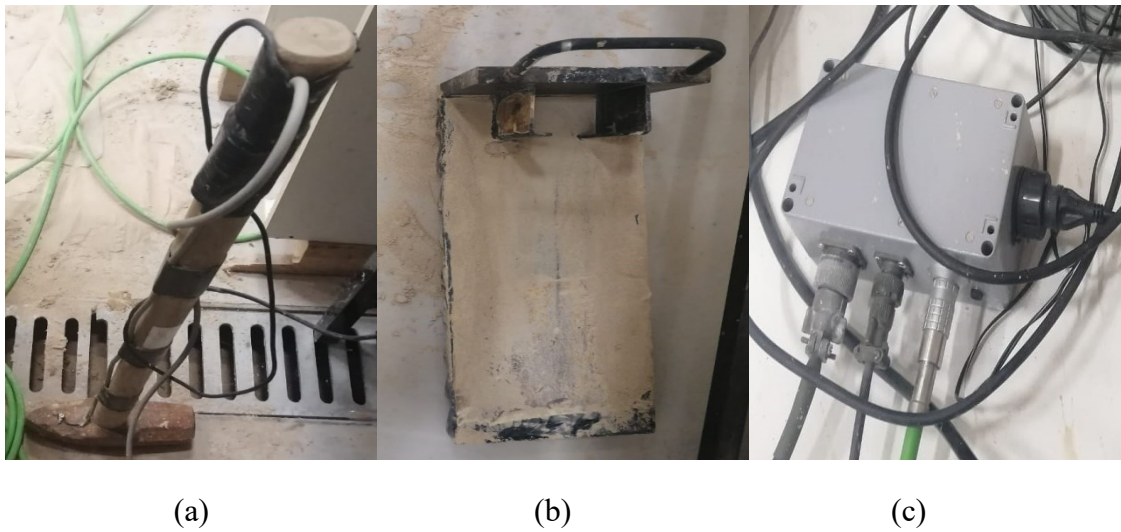


Figure 4.12. (a) Sledgehammer (b) Steel plate (c) Seismic data acquisition box

4.3.2. Test Procedure

SCPT experiments were performed using ASTM D7400 / D7400M-19 and ASTM D5778-20. The CPT probe was stopped at 0.4, 0.8 and 1.2 meters in each experiment and hit the steel plate with a sledgehammer. Thus, by creating shear waves in these meters,

SCPT was completed for 13 experiments. SCPT experiment conducted in the laboratory is given in Figure 4.13.



Figure 4.13. The SCPT experiment performed in the laboratory

The shear wave velocity is calculated by dividing the distance of the wave formed by hitting the steel plate with a sledgehammer at two different depths to the seismometer at these depths by the difference between the two times. The cross-correlation method is used to calculate shear wave velocity. The cross-correlation method is more advantageous than other methods. These advantages can be listed as follows: Works well with low signals, more shear wave velocity estimation, less human resource requirement, fast results, using the whole wave signal instead of a single point.

The cross-correlation method uses the entire signal of shear waves at 0.4 - 0.8 m and 0.8 - 1.2 m depths to measure the time at which the low signal should be shifted to the high signal. After all, signals are shifted, the sum of the products of the amplitudes (cross-correlation) of these signals and the widest time shift on the shifted time graph are used for shear wave velocity calculation. (Campanella et al., 1992; Campanella et al., 1995).

GeoTech SCPT Analysis software was used as shown in Figure 4.14 by applying the cross-correlation method in the experiment.

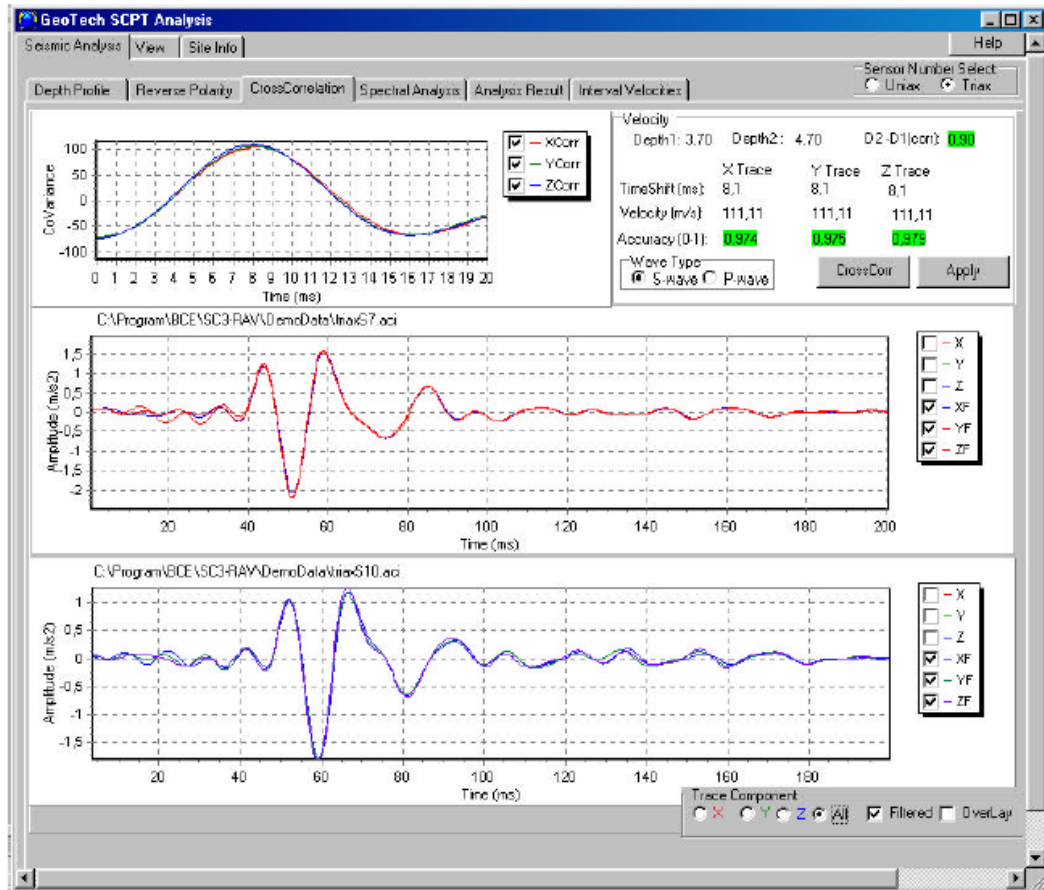


Figure 4.14. GeoTech SCPT Analysis program by performing the Cross-Correlation method

Although seismic CPT tests are performed correctly, there are unwanted noise and body waves in the signals. To avoid this and to get pure shear waves, filtering should be used. In the cross-correlation method used in the Geotech CPT Pro software, a suitable filter was created for the experiments by manually entering the low and high frequency from the bandpass filter option. While entering the filter values, the program automatically changed the correlation values between 0 and 1. Care was taken to ensure accuracy was greater than 0.9. An extensive frequency range may contain noise, and a very narrow frequency range may not represent a wavelet. Therefore, filters with a 3 - 7 ms delay and better representation of wavelets in the frequency range 148 - 333 are used.

4.3.3. SCPT Test Data

Figure 4.15 shows the shear wave velocity data of clean sand, 5%, 15% and 35% silty sands with penetration depth.

D_r is between 15 - 22 for Test 1, between 35 - 50 for Test 2 and between 45 - 65 for Test 3 in clean sand. In Figure 4.15. (a), V_s as 74.07 m/sec for Test 1, V_s as 90 m/sec for Test 2, V_s as 66.7 m/sec at 0.2 m depth and 100 m/sec at 0.44 m depth for Test 3.

D_r is 18 for Test 4, between 23-25 for Test 6 and between 70 - 75 for Test 5 in 5% silty sands. In Figure 4.15. (b), V_s as 71.43 m/sec between 0.4 - 0.8 m depth and 107.69 m/sec between 0.8 - 1.2 m depth for Test 4, V_s as 83.33 m/sec between 0.4 - 0.8 m depth and 100 m/sec between 0.8 - 1.2 m depth for Test 6, V_s as 110 m/sec between 0.4 - 0.8 m depth and 120 m/sec between 0.8 - 1.2 m depth for Test 5.

D_r is between 21 – 23 for Test 7, between 35-40 for Test 8, and between 35-44 for Test 9 in 15% silty sands. In Figure 4.15. (c), V_s as 66.67 m/sec between 0.4 - 0.8 m depth and 100 m/sec between 0.8 - 1.2 m depth for Test 7, V_s as 71.43 m/sec between 0.4 - 0.8 m depth and 87.5 m/sec between 0.8 - 1.2 m depth for Test 8, V_s as 76.92 m/sec between 0.4 - 0.8 m depth and 100 m/sec between 0.8 - 1.2 m depth for Test 9.

D_r is between 35-36 for Test 10, between 34 – 46 for Test 12, and between 30 - 55 for Test 11 in 35% silty sands. 4.15. (d), V_s as 66.67 m/sec between 0.4 - 0.8 m depth and 93.33 m/sec between 0.8 - 1.2 m depth for Test 10, V_s as 83.33 m/sec between 0.4 - 0.8 m depth and 87.5 m/sec between 0.8 - 1.2 m depth for Test 12, V_s as 85.71 m/sec for Test 11.

In general, shear wave velocity increases with increasing depth in clean sands and silty sands. Also, the higher the relative density, the higher the shear wave velocity is. On the other hand, shear wave velocity decreases as fines content increases.

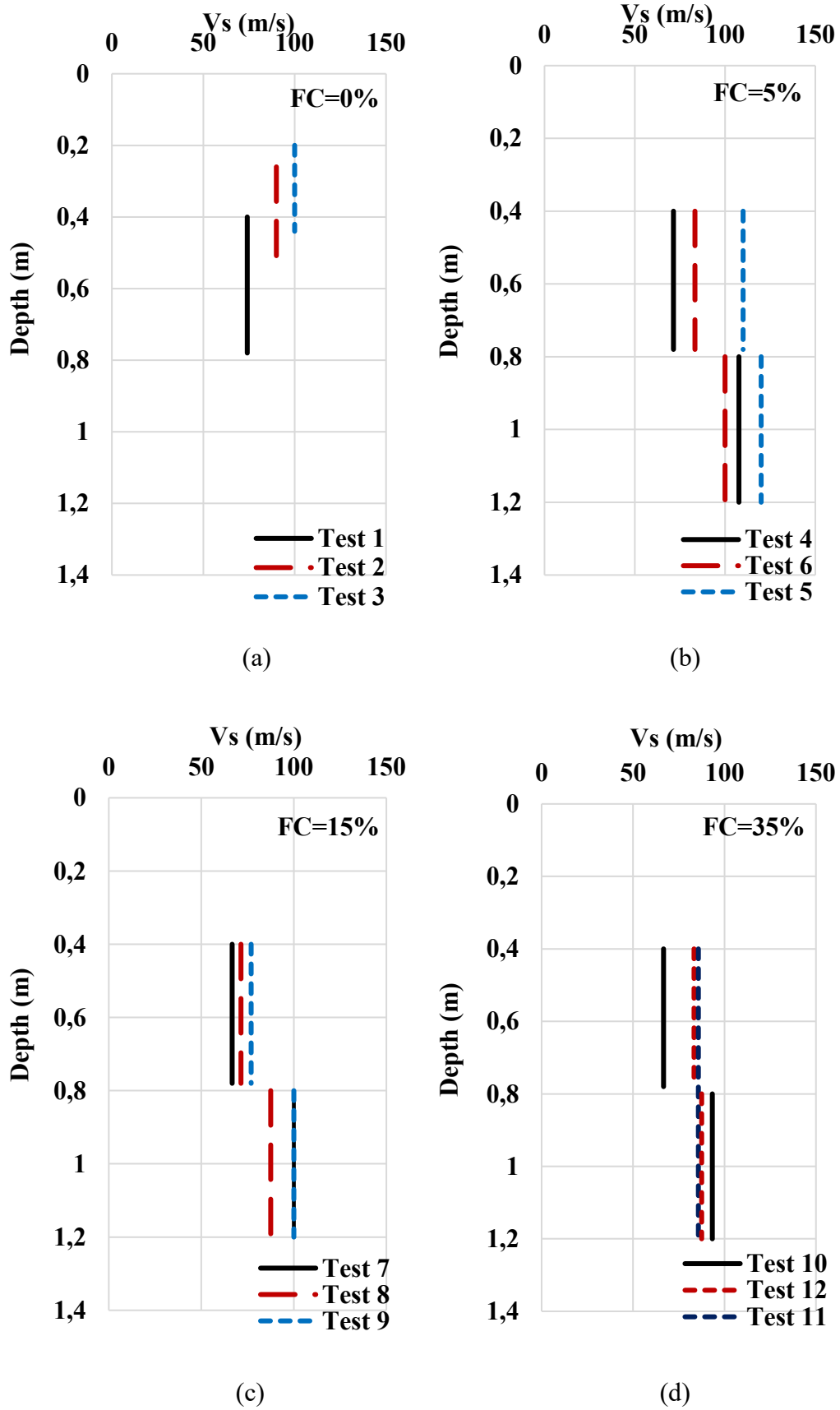
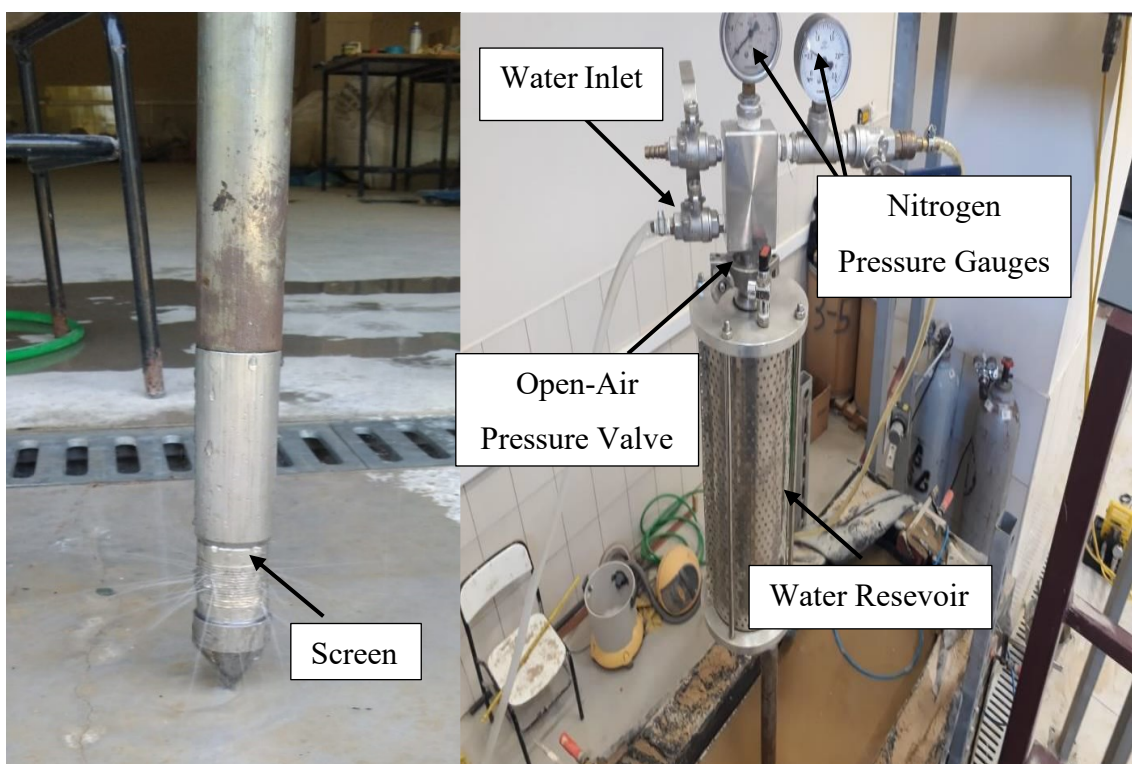


Figure 4.15. The shear wave velocity data of (a) clean sand (b) 5% silty sand (c) 15% silty sand (d) 35% silty sands, with the penetration depth.

4.4. Direct Push Permeability Test (DPPT)

A permeability test was performed to calculate hydraulic conductivity. These experiments were carried out to obtain direct permeability of the soil at 0.4, 0.8 and 1.2 meters of depths. A permeameter was created by adding a 10 cm² base area and a 60-degree conical tip screen probe to the CPT rod. As shown in Figure 4.16 (a), a filter is placed at the cone tip to allow water to flow out. There is a 30 cm high cylindrical water reservoir, water inlet to the reservoir and reservoir valve on the rod. It also has a nitrogen gas inlet, inlet valve, pressure gauges and open-air pressure valve to save time, as shown in Fig.4.16 (b).



(a)

(b)

Figure 4.16. (a) A filter is placed at the cone tip to allow water to flow out (b) Cylindrical water reservoir, water and gas inlet and valves

DPPT has been brought to the given depths and fixed. The time elapsed at a certain height change was measured by filling the cylindrical water reservoir with water. The direct push permeability test obtains manual water flow measurement as the volume discharge over time under constant pressure.

Permeability is calculated using the equations below (Lee et al., 2008):

$$k = \frac{Q}{4\pi\Delta h a_s} \quad (4.1)$$

$$a_s = \sqrt{\frac{1}{2}al} \quad (4.2)$$

where k is permeability, Q is volumetric flow, Δh is the excess head, a_s is the effective radius of the spherical injection zone, a is the radius of the screen, and l is the screen's length.

4.4.1. DPPT Test Data

Table 4.1. shows modified DPPT permeability data (Saritas, 2021). Permeability is in the order of 10^{-4} in clean sand and 5% silty sand, 10^{-6} in 15% silty sand and 10^{-7} in 35% silty sand. Although the k value of clean sand is in the same order compared to 5% silty sand, it is higher or even doubles in dense soils. Permeability of 15% silty sands is two orders lower than 5% silty sands, and permeability of 35% silty sands is one order lower than 15% silty sands.

Table 4.1. The modified DPPT permeability data. (Saritas, 2021)

Test No.	FC	Depth	DPPT
			Permeability, k
-	%	m	m/sec
T1	0	0,4	0,000431
		0,8	0,000437
		1,2	0,000452
T2	0	0,26	0,000392
		0,52	0,000347
T3	0	0,2	0,000362
		0,44	0,000302
T4	5	0,4	3,96E-04
		0,8	3,96E-04
		1,2	3,96E-04
T5	5	0,4	1,88E-04
		0,8	1,68E-04
		1,2	1,80E-04
T6	5	0,4	3,68E-04
		0,8	3,72E-04
		1,2	3,76E-04
T7	15	0,4	3,31E-06
		0,8	3,34E-06
		1,2	3,37E-06
T8	15	0,4	2,80E-06
		0,8	2,80E-06
		1,2	2,95E-06
T9	15	0,4	2,95E-06
		0,8	2,68E-06
		1,2	2,95E-06
T10	35	0,4	3,84E-07
		0,8	3,84E-07
		1,2	3,90E-07
T11	35	0,4	2,88E-07
		0,8	4,20E-07
		1,2	3,36E-07
T12	35	0,4	3,24E-07
		0,8	3,96E-07
		1,2	3,84E-07
T13	35	0,3	3,30E-07
		0,6	2,70E-07

4.5. Conclusion

The CPT, SCPT and DPPT experiments were performed on clean sand, 5%, 15% and 35% silty sand. q_c and u_2 data for CPT, V_s data for SCPT and k data for DPPT with Figures and Table for loose soil, medium dense soil and dense soil was created and presented above. In general, it is observed that as the silt ratio increases, the measured q_c , V_s and k values decrease. On the other hand, u_2 increases. The following Chapter presents the results of the tests.

CHAPTER 5

RESULTS OF THE TESTS

5.1. Introduction

In the experiments conducted on the clean sand and silty sands using CPTu, the effect of fines content on q_{c1N} and $\Delta u/\sigma_{vo}'$ over T was investigated. Studies examining the effect of fines content on q_{c1N} and $\Delta u/\sigma_{vo}'$ are presented in the literature in the second Chapter. Despite increasing studies in recent years, the effect of fines content is not yet known. In this Chapter, first, k , m_v and c_h of clean sand and silty sands are compared at different relative densities given. Then, the effect of relative densities on q_{c1N} and $\Delta u/\sigma_{vo}'$ are examined in clean sand and silty sands. Finally, T's effect with different v and c_h values on q_{c1N} and $\Delta u/\sigma_{vo}'$ are examined. The transition values of drainage conditions in T found in these studies were compared with literature studies.

5.2. m_v , k and c_h of Clean Sand and Silty Sands at Different Relative Densities

The effects of fine on q_{c1N} and $\Delta u/\sigma_{vo}'$ will be studied. For this, first of all, m_v , k and c_h of clean sand and silty sand should be examined. The effect of fines content on m_v , k and c_h has been investigated in limited studies (Shenthan, 2001; Thevanayagam and Martin, 2002; Ecemis, 2008; Bandini and Sathiskumar, 2009; Huang, 2015). The coefficient of consolidation calculated with k and m_v is an essential parameter in the generation and dissipation time of excess pore water pressure in cone penetration.

The coefficient of consolidation was calculated by the formula below:

$$c_h = \frac{k}{\gamma_w m_v} \quad (5.1)$$

where k is the permeability of the soil, γ_w is the unit weight of water, and m_v is the coefficient of volume compressibility.

The coefficient of volume compressibility was calculated based on shear wave velocity as follows:

$$m_v = \frac{3(1 - 2\nu)}{E} \quad (5.2)$$

$$E = 2G(1 + \nu) \quad (5.3)$$

$$G = V_s^2 \rho \quad (5.4)$$

where E is the modulus of elasticity and ν is the Poisson's ratio in Equation 5.2., G is the shear modulus in Equation 5.3; V_s is the shear wave velocity and ρ is the soil's density in Equation 5.4. Using Equations 5.2, 5.3 and 5.4, the following formula is derived.

$$m_v = \frac{1.5(1 - 2\nu)}{(V_s^2 \rho)(1 + \nu)} \quad (5.5)$$

In Table 5.1, m_v values calculated according to Equation 5.5 are given at different depths and different relative densities for each test. The Poisson's ratio used in the equation was taken as 0.25. Calculation of the density of the samples is given in Chapter 3. Shear wave velocities were obtained from SCPT experiments. Relative density was calculated according to the water content, and these calculations are given in Chapter 3.

Table 5.1. m_v values calculated according to Equation 5.5 at different depths and different relative densities

Test No.	FC	Depth	Density	V_s	Average D_r	m_v
-	%	m	kg/m ³	m/sec	%	1/kPa
T1	0	0,4	1899	74,07	22	5,76E-05
		0,8		74,07	20	5,76E-05
		1,2		74,07	15	5,76E-05
T2	0	0,26	1933	90	35	3,83E-05
		0,52		90	50	3,83E-05
T3	0	0,2	2059	66,7	45	6,55E-05
		0,44		100	65	2,91E-05
T4	5	0,4	1828	71,43	18	6,43E-05
		0,8		107,69	18	2,83E-05
		1,2		107,69	18	2,83E-05
T5	5	0,4	1960	110	70	2,53E-05
		0,8		120	75	2,13E-05
		1,2		120	72	2,13E-05
T6	5	0,4	1889	83,33	25	4,57E-05
		0,8		100	24	3,18E-05
		1,2		100	23	3,18E-05
T7	15	0,4	2052	66,67	23	6,58E-05
		0,8		100	22	2,92E-05
		1,2		100	21	2,92E-05
T8	15	0,4	1955	71,43	40	6,02E-05
		0,8		87,5	40	4,01E-05
		1,2		87,5	35	4,01E-05
T9	15	0,4	1935	76,92	35	5,24E-05
		0,8		100	44	3,1E-05
		1,2		100	35	3,1E-05
T10	35	0,4	1943	66,67	36	6,95E-05
		0,8		93,33	36	3,54E-05
		1,2		93,33	35	3,54E-05
T11	35	0,4	2083	85,71	52	3,92E-05
		0,8		85,71	30	3,92E-05
		1,2		85,71	44	3,92E-05
T12	35	0,4	2206	83,33	46	3,92E-05
		0,8		87,5	34	3,55E-05
		1,2		87,5	36	3,55E-05
T13	35	0,3	2010	85,71	45	4,06E-05
		0,6		85,71	55	4,06E-05

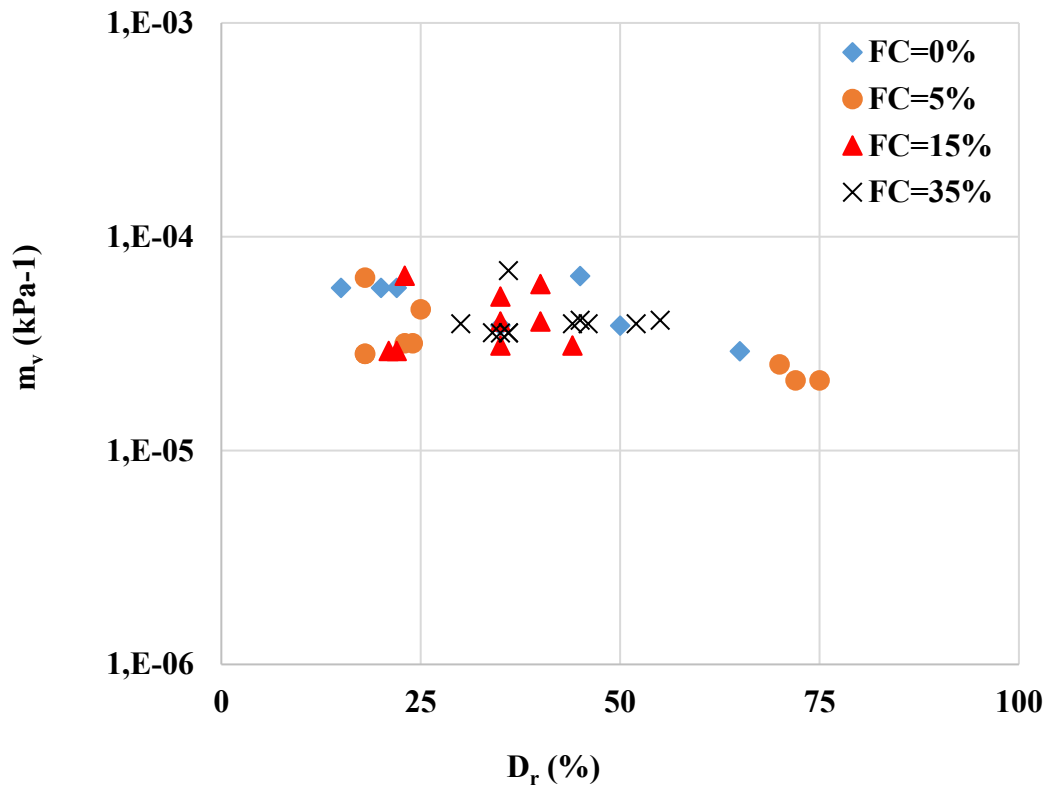


Figure 5.1. The relative density versus coefficient of compressibility in clean sand and silty sands

The relative density and coefficient of volume compressibility of clean sand 5%, 15%, 35% silty sand are compared in Figure 5.1. It is close to each other in m_v 10^{-5} band for loose, medium-dense and dense soils in clean sand and silty sands. (Bandini and Sathiskumar, 2009) reported that the effect of silt content from 0 to 25% on m_v is much low, and the calculated m_v are in the same order. m_v values were calculated with different V_s and ρ variables. V_s and ρ variables were found to be close to each other for all experiments. Therefore, m_v values for sand and silty sands are in the same order.

In Table 5.2, c_h values calculated according to Equation 5.1 are given at different depths and different relative densities in the clean sand and silty sands.

Table 5.2. c_h values at different depths and different relative densities

Test No.	FC	Depth	m_v	k	Average D_r	c_h
-	%	m	1/kPa	m/sec	%	cm^2/sec
T1	0	0,4	5,76E-05	0,000431	22	7,63E+03
		0,8	5,76E-05	0,000437	20	7,73E+03
		1,2	5,76E-05	0,000452	15	8,00E+03
T2	0	0,26	3,83E-05	0,000392	35	1,04E+04
		0,52	3,83E-05	0,000347	50	9,23E+03
T3	0	0,2	6,55E-05	0,000362	45	5,63E+03
		0,44	2,91E-05	0,000302	65	1,06E+04
T4	5	0,4	6,43E-05	3,96E-04	18	6,28E+03
		0,8	2,83E-05	3,96E-04	18	1,43E+04
		1,2	2,83E-05	3,96E-04	18	1,43E+04
T5	5	0,4	2,53E-05	1,88E-04	70	7,57E+03
		0,8	2,13E-05	1,68E-04	75	8,06E+03
		1,2	2,13E-05	1,80E-04	72	8,63E+03
T6	5	0,4	4,57E-05	3,68E-04	25	8,20E+03
		0,8	3,18E-05	3,72E-04	24	1,19E+04
		1,2	3,18E-05	3,76E-04	23	1,21E+04
T7	15	0,4	6,58E-05	3,31E-06	23	5,13E+01
		0,8	2,92E-05	3,34E-06	22	1,16E+02
		1,2	2,92E-05	3,37E-06	21	1,18E+02
T8	15	0,4	6,02E-05	2,80E-06	40	4,74E+01
		0,8	4,01E-05	2,80E-06	40	7,12E+01
		1,2	4,01E-05	2,95E-06	35	7,50E+01
T9	15	0,4	5,24E-05	2,95E-06	35	5,74E+01
		0,8	3,10E-05	2,68E-06	44	8,81E+01
		1,2	3,10E-05	2,95E-06	35	9,70E+01
T10	35	0,4	6,95E-05	3,84E-07	36	5,63E+00
		0,8	3,54E-05	3,84E-07	36	1,10E+01
		1,2	3,54E-05	3,90E-07	35	1,12E+01
T11	35	0,4	3,92E-05	2,88E-07	52	7,49E+00
		0,8	3,92E-05	4,20E-07	30	1,09E+01
		1,2	3,92E-05	3,36E-07	44	8,74E+00
T12	35	0,4	3,92E-05	3,24E-07	46	8,43E+00
		0,8	3,55E-05	3,96E-07	34	1,14E+01
		1,2	3,55E-05	3,84E-07	36	1,10E+01
T13	35	0,3	4,06E-05	3,30E-07	45	8,28E+00
		0,6	4,06E-05	2,70E-07	55	6,77E+00

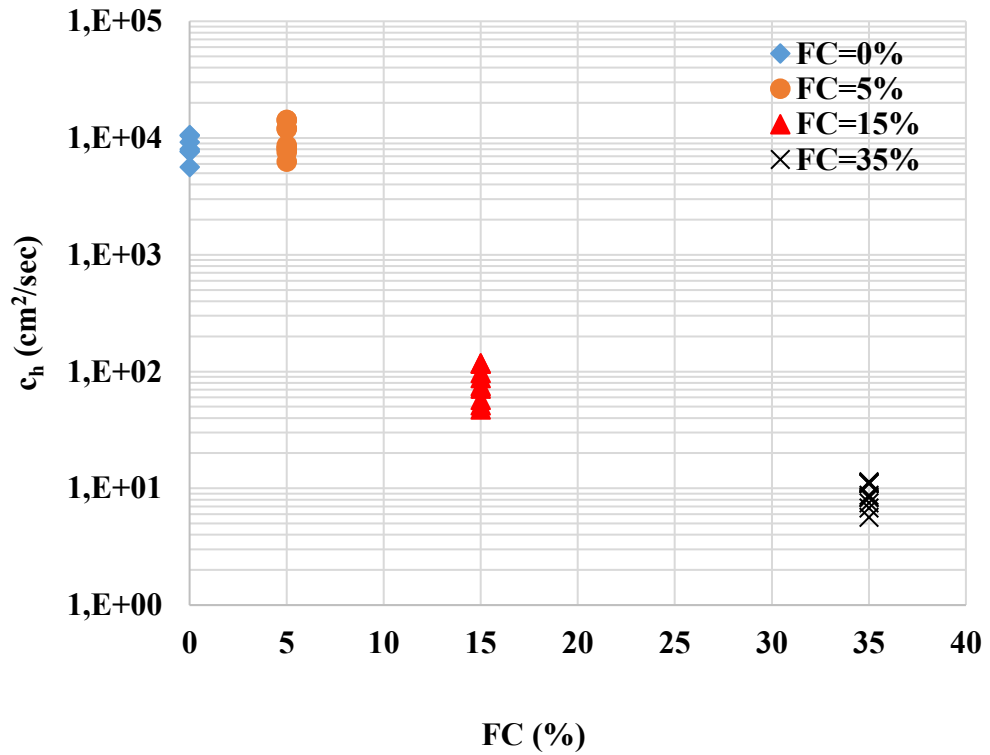


Figure 5.2. c_h values of clean sand, 5%, 15%, and 35% silty sands according to fines content

Figure 5.2 shows that c_h values of clean sand, 5%, 15%, and 35% silty sands are given according to fines content. c_h values of clean sand are in the range of 5,63E+03 to 1,06E+04. The c_h values of 5% silty sands vary between 6,28E+03 and 1,43E+04. c_h values of 15% silty sands are in the range of 4,74E+01 to 1,18E+02. The c_h values of 35% silty sands vary between 5,63E+00 and 1,14E+01.

The c_h values of clean sand and 5% silty sand are very close to each other. 15% silty sands have c_h values two orders lower than clean sand and 35% silty sands three orders lower than clean sand.

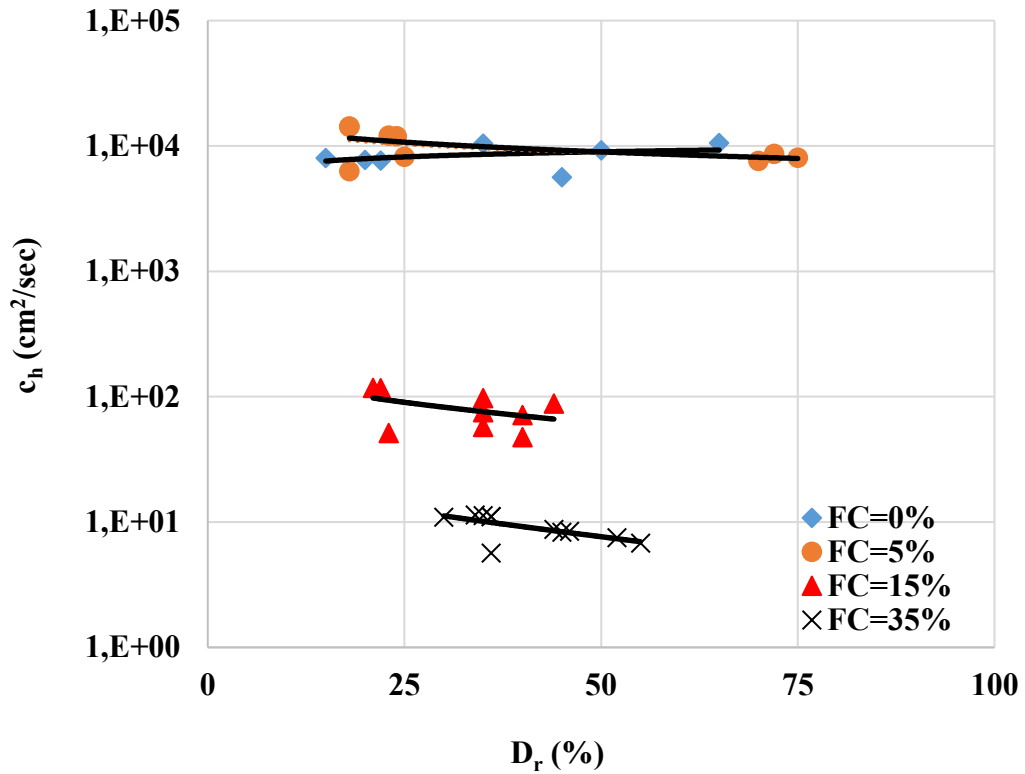


Figure 5.3. c_h values with respect to relative densities in fines content

In Figure 5.3, c_h values are compared to relative densities in fines content. The c_h values of clean sand and 5% silty sand at different relative densities such as 25%, 50% and 75% are almost close. However, when comparing clean sand with 15% and 35% silty sands, the difference between c_h values is very high.

c_h values of clean sand and silty sands have been examined basically on k and m_v values. The fines content in clean sand and silty sands has no significant effect on m_v . The main reason for c_h values decreasing with increasing fines content is the significant decrease between k values. While the k values of clean sand and 5% silty sand are close to each other, the reduced pore size with increased fines content up to 15% and 35% significantly reduces the k -values.

The decreasing k values in 15% and 35% silty sands compared to clean sand are factors on these silty sands' lower c_h values. Since the fines content increase in 15% and 35% silty sands has lower c_h values than clean sands, the excess pore water pressure generated during cone penetration has a significant effect on the dissipation time. Dissipation of

excess pore water pressure takes a long time due to decreasing c_h values with fines content is an essential factor that causes different drainage conditions.

5.3. Effect of Fines Content and Relative Density on Normalized Cone Penetration Resistance and Normalized Excess Pore Water Pressure

Normalized cone penetration resistance and normalized excess pore water pressure were studied at different relative densities in clean sand and 5%, 15% and 35% silty sands.

Normalized cone penetration resistance and normalized excess pore water pressure are given in Table 5.3. q_{c1N} was calculated from Equations 2.1, 2.2 and 2.3 given in Chapter 2. $\Delta u/\sigma_{v0}'$ was calculated from Equation 2.4 given in Chapter 2. The parameters used to calculate q_{c1N} and $\Delta u/\sigma_{v0}'$ are given in Table 5.3.

Relative density compared to normalized cone penetration resistance for different fines contents in clean sand and silty sands in Figure 5.4. The data obtained from the experiments are marked with trend lines in the graph. According to the graph, q_{c1N} increases as the relative density increases in all clean sand, 5%, 15% and 35% silty sands. The greater the fines content at the given relative density, the lower q_{c1N} is. Increasing fines content significantly affects the normalized cone penetration resistance.

Relative density compared to the normalized excess pore water pressure for different fines content in clean sand and silty sand in Figure 5.5. The data obtained from the experiments are marked with trend lines in the graph. Normalized excess pore water pressure decreases as the relative density increases in clean sand and sands with 5%, 15% and 35% silt. No more normalized excess pore water pressure relationship could be established with respect to the fines content at the given relative density.

Table 5.3. q_{cIN} and $\Delta u/\sigma_{vo}'$, the parameters used to calculate q_{cIN} and $\Delta u/\sigma_{vo}'$

Test No.	FC	Depth	σ_{vo}'	q_c	u_2	m	C_n	Average D_r	q_{cIN}	$\Delta u/\sigma_{vo}'$
-	%	m	kPa	MPa	MPa	-	-	%	-	
T1	0	0,4	3,12	0,231	0,0043	0,67	10,19	22	24	0,12
		0,8	6,08	0,272	0,0086	0,68	6,71	20	18	0,12
		1,2	9,28	0,225	0,0126	0,71	5,35	15	12	0,09
T2	0	0,26	1,89	0,481	0,0027	0,60	10,89	35	52	0,08
		0,52	3,46	1,297	0,0057	0,52	5,82	50	75	0,17
T3	0	0,2	1,61	0,629	0,0019	0,55	9,67	45	61	-0,04
		0,44	3,56	1,857	0,0043	0,45	4,42	65	82	0,00
T4	5	0,4	2,59	0,085	0,0046	0,69	12,45	18	11	0,26
		0,8	5,03	0,177	0,0092	0,69	7,87	18	14	0,27
		1,2	7,28	0,128	0,0136	0,69	6,10	18	8	0,25
T5	5	0,4	6,64	2,324	0,0006	0,42	3,12	70	72	-0,50
		0,8	9,05	3,167	0,0056	0,39	2,57	75	81	-0,25
		1,2	10,55	2,769	0,0078	0,41	2,51	72	69	-0,38
T6	5	0,4	3,38	0,105	0,0038	0,65	9,16	25	10	-0,04
		0,8	5,88	0,317	0,0083	0,66	6,47	24	21	0,08
		1,2	8,68	0,518	0,0125	0,66	5,07	23	26	0,08
T7	15	0,4	2,2	0,073	0,005	0,66	12,62	23	9	0,49
		0,8	4,1	0,095	0,0103	0,67	8,48	22	8	0,60
		1,2	7,18	0,111	0,0144	0,67	5,91	21	7	0,37
T8	15	0,4	2,84	0,412	0,0042	0,58	7,77	40	32	0,10
		0,8	4,64	0,581	0,0094	0,58	5,86	40	34	0,33
		1,2	7,44	0,603	0,0136	0,60	4,77	35	29	0,25
T9	15	0,4	4,35	0,367	0,0027	0,60	6,59	35	24	-0,28
		0,8	4,55	0,544	0,0095	0,55	5,55	44	30	0,36
		1,2	6,75	0,559	0,0143	0,60	5,06	35	28	0,37
T10	35	0,4	4,67	0,247	0,0024	0,60	6,22	36	15	-0,33
		0,8	11,87	0,44	0,0022	0,60	3,56	36	16	-0,48
		1,2	18,22	0,468	0,0025	0,60	2,79	35	13	-0,51
T11	35	0,4	14,5	0,836	0,0075	0,51	2,69	52	23	-0,79
		0,8	5,4	0,222	0,0086	0,63	6,25	30	14	0,14
		1,2	5,8	0,394	0,0152	0,55	4,85	44	19	0,59
T12	35	0,4	6,82	0,506	0,0002	0,54	4,31	46	22	-0,55
		0,8	4,02	0,266	0,01	0,61	7,03	34	19	0,54
		1,2	6,27	0,439	0,0144	0,60	5,22	36	23	0,42
T13	35	0,3	4,05	0,265	0,0012	0,55	5,82	45	15	-0,43
		0,6	8	0,806	0,0025	0,50	3,51	55	28	-0,42

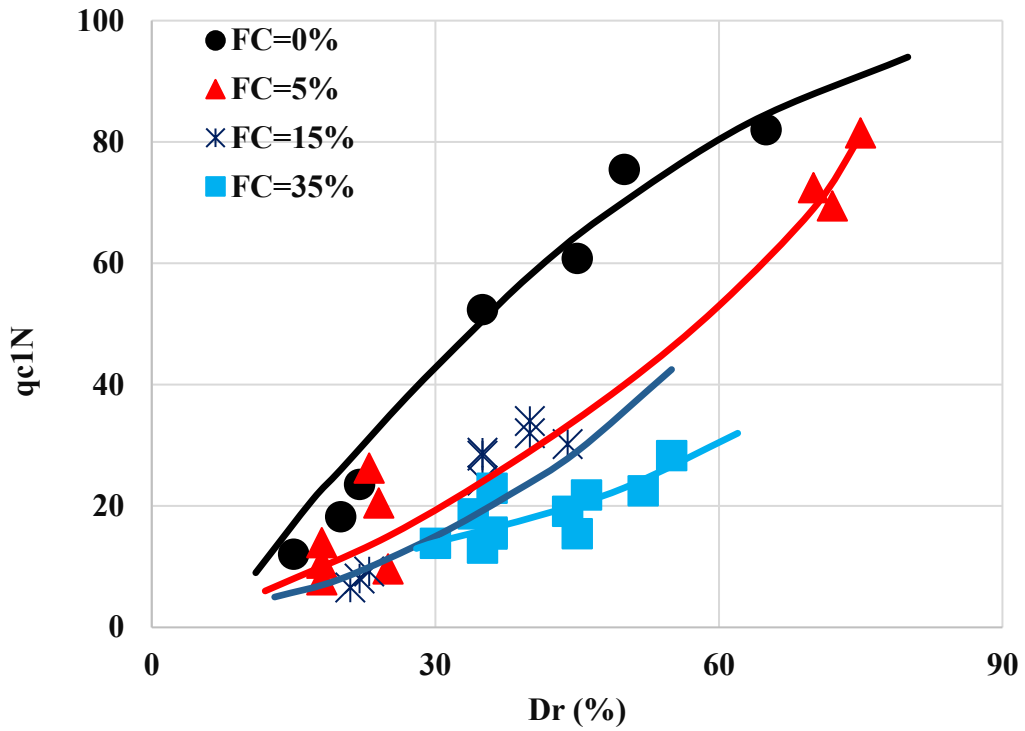


Figure 5.4. Relative density versus normalized cone penetration resistance in clean sand and 5%, 15% and 35% silty sands

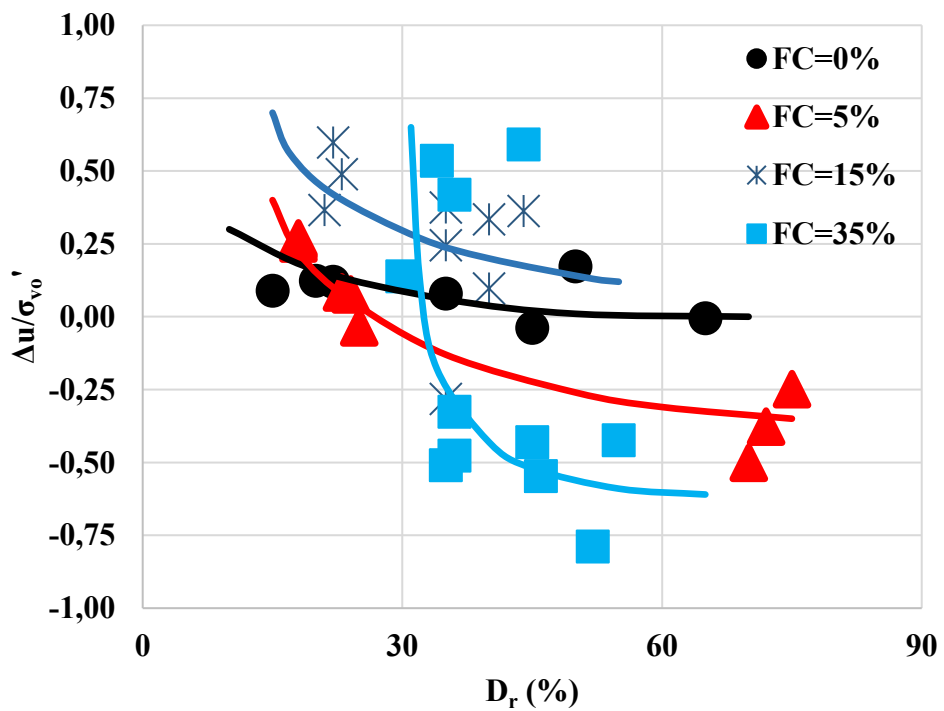


Figure 5.5. Relative density versus normalized excess pore water pressure in clean sand and 5%, 15% and 35% silty sands

5.4. Effect of Coefficient of Consolidation and T on q_{c1N} and $\Delta u/\sigma_{vo}'$

The important difference between the k and c_h values of clean sand and silty sands is examined in Chapter 5.1. As the fines content increases, a significant decrease is observed in the c_h values of 15% and 35% silty sands. Ecemis (2008) reported that this reduction resulted from less effective stress around the probe during cone penetration. The fact that 15% and 35% silty sands have 2-3 orders lower c_h values, respectively, compared to clean sands and the excess pore water pressure generated in CPT penetration affects the slower dissipation time. Different dissipation times lead to different drainage conditions during the loading at cone penetration of clean sand and silty sands. Studies conducted to examine the effect of c_h value on q_{c1N} and $\Delta u/\sigma_{vo}'$ have been suggested to examine its effect over T.

$$T = \frac{v * d}{c_h} \quad (5.6)$$

where T is the normalized penetration rate, v is the penetration rate, d is the diameter of the cone, and c_h is the coefficient of consolidation (Finnie and Randolph, 1994; House et al., 2001; Randolph and Hope, 2004; Chung et al., 2006; Kim et al., 2008; Ecemis, 2008).

The penetration rate in the CPT experiments ranged from 0.8 to 1.5 cm/sec and the cone diameter was 35.7 mm. Table 5.4 shows T and its parameters (v, c_h), q_{c1N} and $\Delta u/\sigma_{vo}'$ values at different depths and different relative densities in clean sand and 5%, 15% and 35% silty sands.

Table 5.4. T and its parameters (v , c_h), q_{c1N} and $\Delta u/\sigma_{vo}'$ values at different depths and different relative densities in clean sand and 5%, 15% and 35% silty sands.

Test No.	FC	Depth	Relative Density D_r	CPT Penetration Velocity v	c_h	Average D_r	q_{c1N}	$\Delta u/\sigma_{vo}'$	Normalized Penetration Rate $T=vd/c_h$
-	%	m	%	cm/sec	cm ² /sec	%	-	-	-
T1	0	0,4	18	1,4	7,63E+03	22	24	0,12	6,6E-04
		0,8		1,4	7,73E+03	20	18	0,12	6,5E-04
		1,2		1,5	8,00E+03	15	12	0,09	6,7E-04
T2	0	0,26	55	1,3	1,04E+04	35	52	0,08	4,4E-04
		0,52		1,2	9,23E+03	50	75	0,17	4,6E-04
T3	0	0,2	83	1,3	5,63E+03	45	61	-0,04	8,2E-04
		0,44		1,2	1,06E+04	65	82	0,00	4,1E-04
T4	5	0,4	18	1,4	6,28E+03	18	11	0,26	8,0E-04
		0,8		1,4	1,43E+04	18	14	0,27	3,5E-04
		1,2		1,5	1,43E+04	18	8	0,25	3,8E-04
T5	5	0,4	77	1,0	7,57E+03	70	72	-0,50	4,7E-04
		0,8		0,8	8,06E+03	75	81	-0,25	3,5E-04
		1,2		0,8	8,63E+03	72	69	-0,38	3,3E-04
T6	5	0,4	31	1,2	8,20E+03	25	10	-0,04	5,2E-04
		0,8		1,2	1,19E+04	24	21	0,08	3,6E-04
		1,2		1,1	1,21E+04	23	26	0,08	3,3E-04
T7	15	0,4	21	1,1	5,13E+01	23	9	0,49	7,7E-02
		0,8		1,1	1,16E+02	22	8	0,60	3,4E-02
		1,2		1,1	1,18E+02	21	7	0,37	3,3E-02
T8	15	0,4	38	1,2	4,74E+01	40	32	0,10	9,0E-02
		0,8		1,1	7,12E+01	40	34	0,33	5,5E-02
		1,2		1,0	7,50E+01	35	29	0,25	4,8E-02
T9	15	0,4	46	1,3	5,74E+01	35	24	-0,28	8,1E-02
		0,8		1,3	8,81E+01	44	30	0,36	5,3E-02
		1,2		1,3	9,70E+01	35	28	0,37	4,8E-02
T10	35	0,4	32	1,4	5,63E+00	36	15	-0,33	8,9E-01
		0,8		1,3	1,10E+01	36	16	-0,48	4,2E-01
		1,2		1,3	1,12E+01	35	13	-0,51	4,1E-01
T11	35	0,4	48	1,3	7,49E+00	52	23	-0,79	6,2E-01
		0,8		1,4	1,09E+01	30	14	0,14	4,6E-01
		1,2		1,4	8,74E+00	44	19	0,59	5,7E-01
T12	35	0,4	23	1,3	8,43E+00	46	22	-0,55	5,5E-01
		0,8		1,4	1,14E+01	34	19	0,54	4,4E-01
		1,2		1,3	1,10E+01	36	23	0,42	4,2E-01
T13	35	0,3	79	1,4	8,28E+00	45	15	-0,43	6,0E-01
		0,6		1,3	6,77E+00	55	28	-0,42	6,9E-01

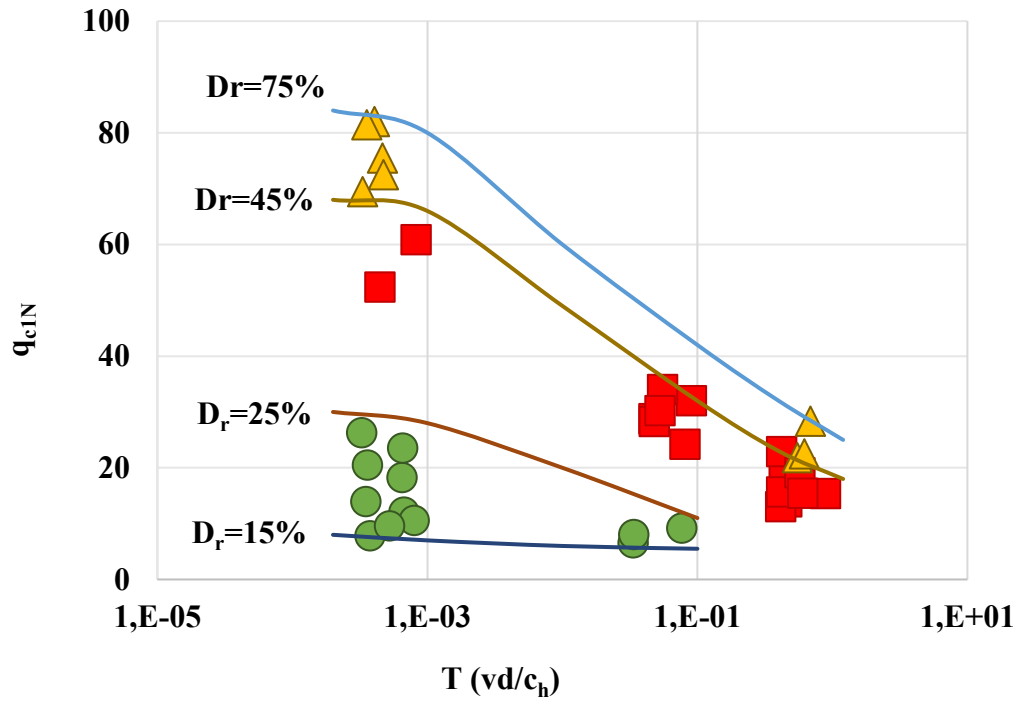


Figure 5.6. Comparison of T with q_{cIN} at a given relative densities

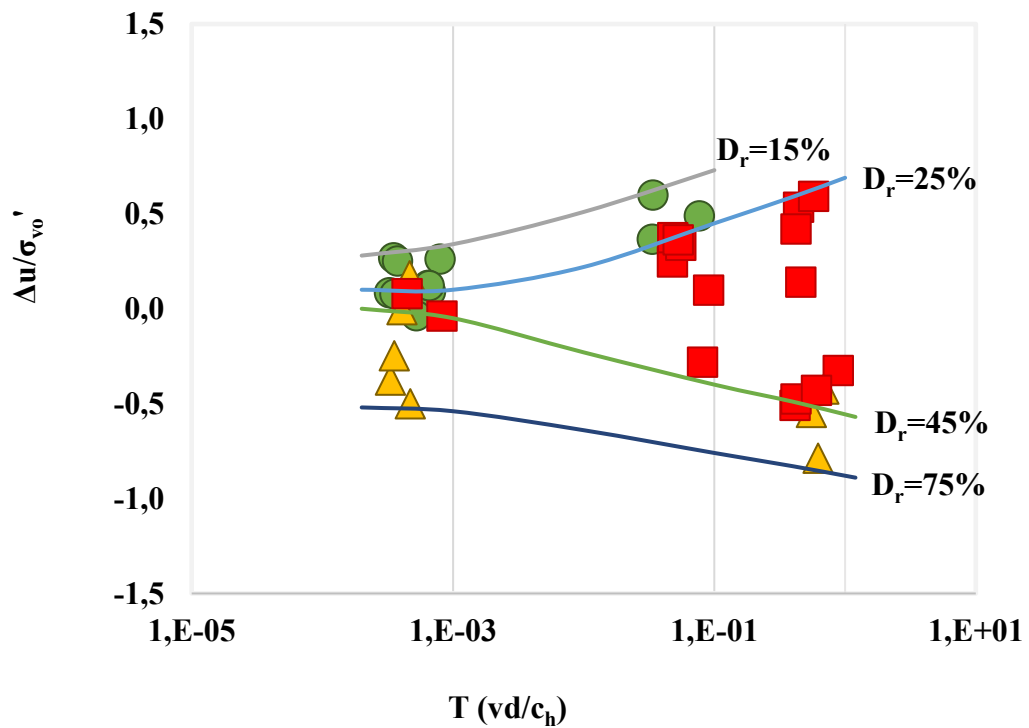


Figure 5.7. Comparison of T with $\Delta u/\sigma_{vo}'$ at a given relative densities

Figures 5.6 and 5.7 compare T with q_{c1N} and $\Delta u/\sigma_{vo}'$. Point data obtained from clean sand and silty sands tests vary in the relative density ranges of 15-25% (loose), 25-45% (medium) and 45-75% (dense) and these lower and upper limits are $D_r = 15\%$, $D_r = 25\%$, $D_r = 45\%$ and $D_r = 75\%$ drawn as trendline.

In Figure 5.6, at $D_r = 15-25\%$, T varies between $3,3E-04$ and $7,7E-02$, and q_{c1N} varies between 7 and 26. At $D_r = 25-45\%$, T varies between $4,4E-04$ and $8,9E-01$, and q_{c1N} varies between 13 and 61. At $D_r = 45-75\%$, T varies between $3,3E-04$ and $6,9E-01$, and q_{c1N} varies between 22 and 82. While a significant decrease was observed in the q_{c1N} values at $D_r = 45-75\%$ (dense) and $D_r = 25-45\%$ (medium), a lesser decrease was observed at $D_r = 15-25\%$ (loose). In Figure 5.6, q_{c1N} decreases as T increases at given relative densities. At the given relative densities, the change in T at $T < 10^{-3}$ values affects q_{c1N} slightly, while q_{c1N} decreases significantly with the increase of T at $T > 10^{-3}$ values.

In Figure 5.7, at $D_r = 15-25\%$, T varies between $3,3E-04$ and $7,7E-02$, and $\Delta u/\sigma_{vo}'$ varies between -0.04 and 0.6. At $D_r = 25-45\%$, T varies between $4,4E-04$ and $8,9E-01$, and $\Delta u/\sigma_{vo}'$ varies between -0.51 and 0.59. At $D_r = 45-75\%$, T varies between $3,3E-04$ and $6,9E-01$, and $\Delta u/\sigma_{vo}'$ varies between -0.79 and 0.17. In Figure 5.7, at the given relative densities, $\Delta u/\sigma_{vo}'$ is slightly affected at $T < 10^{-3}$ values. As T increases at $T > 10^{-3}$ values, while $\Delta u/\sigma_{vo}'$ increases at $D_r = 15\%$ and $D_r = 25\%$, $\Delta u/\sigma_{vo}'$ decreases at $D_r = 45\%$ and $D_r = 75\%$. As T increases at $D_r = 45-75\%$ range, a significant amount of negative $\Delta u/\sigma_{vo}'$ occurs. Dilative behavior is seen in this dense soil.

Clean sand remained at $T < 10^{-3}$ values, and in clean sand q_{c1N} and $\Delta u/\sigma_{vo}'$ were slightly affected by the change of T . Silty sands remained at $T > 10^{-3}$ values, and in silty sands, q_{c1N} and $\Delta u/\sigma_{vo}'$ were significantly affected by the change of T . Penetration ratio values are between 0.8 and 1.5, and c_h nearly between 10^1 to 10^4 . Both the coefficient of consolidation and the penetration rate are in the time of generation and dissipation of excess pore water pressure at cone penetration and affect drainage conditions. Clean sand remains in drained conditions, and silty sands remain in partially drained conditions. Therefore, different tendency observed in the $T - q_{c1N}$ and $T - \Delta u/\sigma_{vo}'$ relationships of silty sands compared to clean sand.

In this study, the effect of T on q_{c1N} and $\Delta u/\sigma_{vo}'$ was examined. The transition value of T was found to be drained for $T < 10^{-3}$ and partially drained for $T > 10^{-3}$. Looking at the fines content's effect, examining q_{c1N} and $\Delta u/\sigma_{vo}'$ over the T value seems a less erroneous method for determining drainage conditions' transition value. In the literature studies in

Chapter 2, the transition values from drained to partially drained are presented. Accordingly, other researchers found the transition values from drained to partially drained as $T < 0.01$ (Finnie and Randolph, 1994), $T < 0.1$ (House et al., 2001), $T < 0.05$ (Kim et al., 2008), $T < 0.01$ (Ecemis, 2008), $T < 0.05$ (Lehane et al., 2009), $T < 0.01$ (Jaeger et al., 2010) and $T < 0.04$ (Huang, 2015).

5.5. Conclusion

In this Chapter, k , m_v and c_h of clean sand and 5%, 15% and 35% silty sands are compared. The k and c_h values of clean sand and mostly 15% and 35% silty sands are 2-3 order different. Clean sand and silty sands' m_v are in the same order and are close to each other. T from accounted with c_h and v values on q_{c1N} and $\Delta u/\sigma_{vo}'$, it has been observed that clean sand and silty sands show different tendencies. This showed that the normalized cone penetration resistance and normalized excess pore water pressure should be examined with T , not just the silt ratio. From drained to partially drained, the value was found to be 10^{-3} . Clean sands remained in drained conditions, while silty sands remained in partially drained conditions. As T increased in silty sands at given relative densities, q_{c1N} decreased significantly. Also, as T increased in silty sands, while $\Delta u/\sigma_{vo}'$ increased at $D_r = 15\%$ and $D_r = 25\%$, negative excess pore pressure occurred at $D_r = 45\%$ and $D_r = 75\%$. The following Chapter presents the conclusion.

CHAPTER 6

CONCLUSION

To examine the effect of fines content on cone penetration resistance and excess pore water pressure, a total of 13 tests (CPTu, SCPT, DPPT) were carried out in a fixed-wall laminar box fully saturated with water in clean sand and 5%, 15% and 35% silty sands.

Firstly, m_v , k and c_h values of clean sand and silty sand were investigated.

- m_v values of clean sand and silty sands were found to be in the same order and close to each other.
- While the k and c_h values of clean sand and 5% silty sands were found to be close to each other, the k and c_h values of 15% and 35% silty sands were found to be 2-3 orders lower, respectively, compared to clean sand.

Secondly, the effect of the fines content on the normalized cone penetration resistance and normalized excess pore water pressure was investigated with relative densities.

- It has been observed that as the fines content increased in the samples at the given relative densities, the normalized cone penetration resistance decreased significantly. Also, as the relative density increased in clean sand and silty sands, the normalized cone penetration resistance decreased.
- It has been observed that as the relative density increases in clean sand and silty sands, the normalized excess pore water pressure decreases. No relationship could be established between the fines content at the given relative densities and the normalized excess pore water pressure.

Thirdly, q_{c1N} and $\Delta u/\sigma_{v0}'$ were examined over T (considering v and c_h) at different relative densities in clean sand and silty sands.

- Clean sand remained at $T < 10^{-3}$ values, and in clean sand q_{c1N} and $\Delta u/\sigma_{v0}'$ were slightly affected by the change of T .
- Silty sands remained at $T > 10^{-3}$ values, and in silty sands q_{c1N} and $\Delta u/\sigma_{v0}'$ were significantly affected by the change of T . With the increase of T at $T > 10^{-3}$ values:

- While a significant decrease was observed in the q_{c1N} values at $D_r = 45-75\%$ (dense) and $D_r = 25-45\%$ (medium), a lesser decrease was observed at $D_r = 15-25\%$ (loose).
 - While $\Delta u/\sigma_{vo}'$ values increased at $D_r = 15\%$ and $D_r = 25\%$, decreased at $D_r = 45\%$ and $D_r = 75\%$.
- The transition value from drained to partially drained was found to be $T = 10^{-3}$.

Consequently, the difference in fines content leads to very different k and c_h values. Both the coefficient of consolidation (a fundamental soil parameter) and the rate of penetration are in the generation and dissipation time of excess pore water pressure at cone penetration and affect drainage conditions. In clean sand (drained) and silty sand (partially drained) remaining under different drainage conditions, $T - q_{c1N}$ and $T - \Delta u/\sigma_{vo}'$ relationships tend to be very different.

The penetration rate in this study ranged from 0.8 to 1.5 cm/sec. This study can be examined with various penetration rates. The effect of the cone diameter has not been investigated in cone penetration experiments, so it is necessary to investigate the effect of the cone diameter.

REFERENCES

- ASTM D5778-20, “Standard Test Method for Electronic Friction Cone and Piezocone Penetration Testing of Soils.” ASTM International, West Conshohocken, PA, 2020, www.astm.org DOI: 10.1520/D5778-20
- ASTM D6067 / D6067M-17, “Standard Practice for Using the Electronic Piezocone Penetrometer Tests for Environmental Site Characterization and Estimation of Hydraulic Conductivity.” ASTM International, West Conshohocken, PA, 2017, www.astm.org DOI: 10.1520/D6067_D6067M-17
- ASTM D7400 / D7400M-19, “Standard Test Methods for Downhole Seismic Testing.” ASTM International, West Conshohocken, PA, 2019, www.astm.org DOI: 10.1520/D7400_D7400M-19
- Baligh, M.M. and Levadoux, J.N. 1980. “Pore pressure dissipation after cone penetration.” Massachusetts Institute of Technology, Department of Civil Engineering, Cambridge, Mass., Report R80-11.
- Bandini, P., and S. Sathiskumar. 2009. “Effects of silt content and void ratio on the saturated hydraulic conductivity and compressibility of sand-silt mixtures.” *J. Geotech. Geoenviron. Eng.* 135 (12): 1976–80. [https://doi.org/10.1061/\(asce\)gt.1943-5606.0000177](https://doi.org/10.1061/(asce)gt.1943-5606.0000177).
- Boulangier, Ross W. 2003. “High Overburden Stress Effects in Liquefaction Analyses.” *Journal of Geotechnical and Geoenvironmental Engineering* 129 (12). [https://doi.org/10.1061/\(asce\)1090-0241\(2003\)129:12\(1071\)](https://doi.org/10.1061/(asce)1090-0241(2003)129:12(1071)).
- Campanella, R. G., and W. P. Stewart. 1992. “Seismic cone analysis using digital signal processing for dynamic site characterization.” *Can. Geotech. J.* 29 (3): 477-486. <https://doi.org/10.1139/t92-052>.

- Chung, S.F., M. F. Randolph, and J. A. Schneider. 2006. "Effect of penetration rate on penetrometer resistance in clay." *J. Geotech. Geoenviron. Eng.* 132 (9): 1188-1196. [https://doi.org/10.1061/\(asce\)1090-0241\(2006\)132:9\(1188\)](https://doi.org/10.1061/(asce)1090-0241(2006)132:9(1188)).
- Finnie, I. M. S., and M. F. Randolph. 1994. "Punch-through and liquefaction induced failure of shallow foundations on calcareous sediments." In *7th Int. Conf. on the Behaviour of Offshore Structures*, 217-230. Massachusetts : Pergamon.
- Holmsgaard, R., L. B. Ibsen, and B. N. Nelsen. 2016. "Interpretation of Seismic Cone Penetration Testing in Silty Soil." *Electronic Journal of Geotechnical Engineering* 21.15 (Available at [ejge.com](http://www.ejge.com)): 4759–79. <http://www.ejge.com/2016/Ppr2016.0460ma.pdf>.
- House, A. R., J. R. M. S. Oliveira, and M. F. Randolph. 2001. "Evaluating the coefficient of consolidation using penetration tests." *Int. J. Phy. Model. Geotech.* 1 (3): 17–25. <https://doi.org/10.1680/ijpmg.2001.010302>.
- Huang, Q. 2015. "Effect of non-plastic fines on cone resistance in silty sands." Doctoral dissertation, Department of Civil, Structural and Environmental Engineering, State University of New York.
- Jaeger, R. A., J. T. DeJong, R. W. Boulanger, H. E. Low, and M. F. Randolph. 2010. "Variable penetration rate CPT in an intermediate soil." In *Proc., 2nd Int. Symp. on Cone Penetration Testing*.
- Janbu, N. and Senneset, K. 1974. "Effective stress interpretation of in situ static penetration tests." *Proceedings of the European Symposium on Penetration Testing, ESOPT, Stockholm, 2.2*, 181-93.
- Kim, Kwangkyun, Monica Prezzi, Rodrigo Salgado, and Woojin Lee. 2008. "Effect of Penetration Rate on Cone Penetration Resistance in Saturated Clayey Soils." *Journal of Geotechnical and Geoenvironmental Engineering* 134 (8). [https://doi.org/10.1061/\(asce\)1090-0241\(2008\)134:8\(1142\)](https://doi.org/10.1061/(asce)1090-0241(2008)134:8(1142)).

- Kiouis, P. D, G. Z. Voyiadjis, M. T. Tumay. 1988. "A large strain theory and its application in the analysis of the cone penetration mechanism." *Int. J. Num. Analy. Meth. Geomech.* 12 (1): 45-60. <https://doi.org/10.1002/nag.1610120104>.
- Kokusho, T., F. Ito, Y. Nagao, and A. R. Green. 2012. "Influence of non/low-plastic fines and associated aging effects on liquefaction resistance." *J. Geotech. Geoenviron. Eng.* 138 (6): 747–56. [https://doi.org/10.1061/\(asce\)gt.1943-5606.0000632](https://doi.org/10.1061/(asce)gt.1943-5606.0000632).
- Kumar, J. and K. Raju. 2009. "Penetration rate effect on miniature cone tip resistance for different cohesionless material." *Geotech. Test. J.* 32(4): 375-384. <https://doi.org/10.1520/GTJ101828>
- Lee, D. S., D. Elsworth, and R. Hryciw. 2008. "Hydraulic conductivity measurement from on-the-fly uCPT sounding and from visCPT." *J. Geotech. Geoenviron. Eng.* 134 (12): 1720–29. [https://doi.org/10.1061/\(asce\)1090-0241\(2008\)134:12\(1720\)](https://doi.org/10.1061/(asce)1090-0241(2008)134:12(1720)).
- Lehane, B. M., C. D. O'loughlin, C. Gaudin, and M. F. Randolph. 2009. "Rate Effects on Penetrometer Resistance in Kaolin." *Geotechnique* 59 (1). <https://doi.org/10.1680/geot.2007.00072>.
- Lunne, T., P. K. Robertson, and J. J. M. Powell. 1997. "Cone penetration testing in geotechnical practice." Melbourne: Blackie Academic and Professional.
- Markauskas, D., R. Kacianauskas, and R. Katzenbach. 2005. "Simulation of piezocone penetration in saturated porous medium using the FE remeshing technique." *Found. Civ. Environ. Eng.* 6 (6): 103–116.
- Oliveira, J. R. M. S., M. S. S. Almeida, H. P. G. Motta, and M. C. F. Almeida. 2011. "Influence of penetration rate on penetrometer resistance." *J. Geotech. Geoenviron. Eng.* 137 (7): 695-703. [https://doi.org/10.1061/\(asce\)gt.1943-5606.0000480](https://doi.org/10.1061/(asce)gt.1943-5606.0000480).
- Randolph, M. F., and S. Hope. 2004. "Effect of cone velocity on cone resistance and excess pore pressures." In *Proc. of the IS Osaka – Engineering Practice and*

Performance of Soft Deposits, edited by T. Matsui, Y. Tanaka, and M. Mimura, 147–152. Osaka: Yodogawa Kogisha Co. Ltd.

Roy, M., Tremblay, M., Tavenas, F. and La Rochelle, P. 1980. “Induced pore pressures in static penetration tests in sensitive clay.” Proceedings of the 33rd Canadian Geotechnical Conference, Calgary, Preprint Volume, 11.3.1 to 11.3.13.

Schmertmann, J. H. ,1976. “An updated correlation between relative density D_r and Fugro type electric cone bearing q_c .” Contract Report DACW 39-76 M 6646 WES, Vicksburg, Miss.

Schmertmann, J.H. 1978. “Study of feasibility of using Wissa-type piezometer probe to identify liquefaction potential of saturated fine sands.” Waterways Experiment Station, Vicksburg, Technical report, S-78-2.

Schneider, J. A., B. M. Lehane, and F. Schnaid. 2007. “Velocity effects on piezocone tests in normally and overconsolidated clays.” *Int. J. Phy. Model. Geotech.* 7(2): 23–34. <https://doi.org/10.1680/ijpmg.2007.070202>.

Shenthan, T. 2001. “Factors affecting liquefaction mitigation in silty soils using stone columns.” Master of Science Thesis, State University of New York.

Sully, J. P., and R. G. Campanella. 1995. “Evaluation of in situ anisotropy from crosshole and downhole shear wave velocity measurements.” *Geotechnique.* 45 (2): 267-282. [https://doi.org/10.1016/0148-9062\(96\)87034-3](https://doi.org/10.1016/0148-9062(96)87034-3).

Thevanayagam, S. and G.R. Martin. 2002. “Liquefaction in silty soils – screening and remediation issues.” *Soil Dyn. Earth. Eng.* 22 (9-12): 1035-1042. [https://doi.org/10.1016/S0267-7261\(02\)00128-8](https://doi.org/10.1016/S0267-7261(02)00128-8).

Thevanayagam, S., and N. Ecemis. 2008. “Effects of permeability on liquefaction resistance and cone resistance.” *Geotech. Spe. Pub.* 181: 1–11. [https://doi.org/10.1061/40975\(318\)92](https://doi.org/10.1061/40975(318)92).

Van den Berg, V. 1994. "Analysis of soil penetration." Doctoral dissertation, Delft University.

Wissa, A.E.Z., Martin, R.T. and Garlanger, J.E. 1975. "The piezometer probe." Proceedings of the ASCE Specialty Conference on In Situ Measurement of Soil Properties, Raleigh, North Carolina, 1, 53M5, American Society of Engineers (ASCE).

Yi, J. T., S. H. Goh, F. H. Lee, and M. F. Randolph. 2012. "A numerical study of cone penetration in fine grained soils allowing for consolidation effects." *Geotechnique*. 62 (8): 707–719. <https://doi.org/10.1680/geot.8.P.155>.